



Sudan University of Science and Technology

College of Graduate Studies

**Numerical Simulation of Pressure Pulsation
(Case Study of Merowe Hydro Power Plant)**

محاكاة رقمية لنبضات الضغط

(دراسة حالة سد مروى للتوليد المائي)

**A thesis submitted to the College of Graduate Studies, in partial
fulfillment of the requirements of the degree of Doctor of
Philosophy(PhD) in**

Mechanical Engineering - Power

Prepared by ALI AHMED ALI ADAM

Supervisor Dr .TAWFIG AHMED GAMAL ELDIN

April/ 2019

SUDAN UNIVETSITY OF SCIENCE AND TECHNOLOGY

COLLEGE OF GRADUATE STUDIES

DEPATMENT OF MECHANICAL ENGINEERING

NUMERICAL SIMULATION OF PRESSURE PULSATION

(MEROWE HYDRO POWER PLANT CASE STUDY)

This thesis has been approved and accepted in partial fulfillment of the requirements for the degree of doctor of philosophy (Ph. D) in mechanical engineering

Examination Committee

External Examiner

Signature

Dr.: Ali Mohammed Hamdan Adam

.....

Rank: Associate Professor

Date: \ \ 2019

Internal Examiner

Signature

Dr.: Hasan Abdu AllatifOsman

.....

Rank: Associate Professor

Date: \ \ 2019

Supervisor

Signature

Dr.: Tawfig Ahmed Gamal Eldin

.....

Rank: Associate Professor

Date: \ \ 2019

DECLARATION OF THESIS

I declare that this thesis was composed by myself, that the work contained herein is my own except where explicitly stated otherwise in the text, and that this work has not been submitted for any other degree or professional qualification except as specified.

Ali Ahmed Ali Adam

/ / 2019

In my capacity as supervisor of the candidate's thesis, I certify that the above statements are true to the best of my knowledge.

Supervisor: Dr .Tawfig Ahmed Gamal Eldin

..../..../2019

SUDAN UNIVETSITY OF SCIENCE AND TECHNOLOGY

COLLEGE OF GRADUATE STUDIES

ASSIGNING THE COPY-RIGHT

STUDENT NAME:*Ali Ahmed Ali Adam*

TITLE OF THESIS:**NUMERICAL SIMULATION OF PRESSURE
PULSATION**

(MEROWE HYDRO POWER PLANTCASE STUDY)

CONFIDENTIAL

(contains confidential information, access is only possible to the abstract)

OPEN ACCESS

(Thesis to be published as on line full text access)

I acknowledge that Sudan University of Science And Technology reserves right as follows:

1. The project report is the property of Sudan university of Science and Technology
2. The library of Sudan university of Science and Technology has right to make copies of the thesis for purpose of research.
3. The library of Sudan university of Science and Technology has right to make copies of the thesis for academic exchange.

Student/ *Ali Ahmed Ali Adam*

Supervisor Name:Dr. Tawfig Ahmed Gamal Eldin

Signature**Signature**.....

Date.....**Date**

الاية

بِسْمِ اللَّهِ الرَّحْمَنِ الرَّحِيمِ
﴿ أَلَمْ نَشْرَحْ لَكَ صَدْرَكَ ﴾ ﴿ وَوَضَعْنَا عَنكَ وِزْرَكَ ﴾ ﴿ الَّذِي
أَنْقَضَ ظَهْرَكَ ﴾ ﴿ وَرَفَعْنَا لَكَ ذِكْرَكَ ﴾ ﴿ فَإِنَّ مَعَ الْعُسْرِ يُسْرًا ﴾ ﴿
إِنَّ مَعَ الْعُسْرِ يُسْرًا ﴾ ﴿ فَإِذَا فَرَغْتَ فَانصَبْ ﴾ ﴿ وَإِلَىٰ رَبِّكَ
فَارْغَب ﴾ ﴿

صدق الله العظيم

DEDICATION

To my parents

Brother and Sisters

For their love and support

To all whom admired this piece of work

Acknowledgments

I would like to express my profound gratitude to my advisors, Dr Tawfig Ahmed Gamal Eldeen, for their excellent professional guidance and impressive help with all aspects of this thesis. I would also like to thank Dr. Ali Mohammed Hamdan Adam and Dr. Hasan Abdu Allatif Osman for their participation on the examining committee.

I also appreciate the effort from the Merowe Dam Hydro Power, for providing all relevant information and research material to make this thesis a successful and mean full.

Special thanks to my parents and all my good friends for their constant patience, support, and encouragement through all difficult.

Abstract

Part load operations procedures affect pressure pulsations and vortex throughout Francis turbines hydropower plant. The goal of this study to investigate these two phenomena's in the inlet of draft tube operated at part load. Unsteady state flow and three dimensions presents a numerical investigation of water flow and air injection used in the purpose of reducing pressure pulsations and vortex in a typical draft tube of Francis turbines when using different part load discharges were performed using 70% Q_{BEP} , 60% Q_{BEP} and 50% Q_{BEP} at 33 m head in Merowe Dam Hydro power. Two sections were chosen and used during the numerical simulation to predicted pressure pulsations contour. One horizontal section was placed in the draft tube inlet below the turbine. Another was placed in the vertical section. Beside the vortex show was also included in the simulations. ANSYS Fluent was carried out for all the numerical simulation to explore various part load operations. Except for the 50% Q_{BEP} high pressure pulsations and vortex definite during part load operation. Air injection into the draft tube cone wall is installed to reduce the intensity of pressure pulsations and vortex that occur during part load from 12.36% to less than 5%, when injected to 5 bar, data have been compared with guaranteed value. The outcome of this research, demonstrates the potentials and benefits of using air injection in the draft tube to protect the units operation ranges by increasing operation area Hell Chart. Findings show the air can be introduced in various locations to reduce pressure pulsations in harmful operating regions in Merowe Hydro power. Data have been compared with standard values and results reached up to date.

المستخلص

يؤثر التشغيل الجزئي في محطات توليد القدرة المائية التي تعمل بتوربين فرانسيس إلي تكون مساحات ذات نبضات ضغط منخفضة و دوامات في مخرج توربين فرانسيس و مدخل أنبوب التصريف, الهدف من هذه الدراسة هو التخفيف من هاتين الظاهرتين.تمت الحوسبة لنموذج طبق الأصل لأنبوب التصريف توربين فرانسيس ثلاثية الأبعاد يحتوي علي ماء عند جريان غير مستقر و هواء مقترح الغرض منه ضغطه تقليل نبضات الضغط وتكسير الدوامات عند استخدام نسب مختلفة من التصريف الجزئي تتراوح بين 70%, 60% و 50% من التصريف لافضل كفاءة (QBEP) للتوربين و لسمت مقداره 33 متر لسد مروى.اختير مقطعين لتوضيح خارطة نبضات الضغط المنخفضة عند المحاكاة العددية, الأول أفقي عند مخرج التربين و مدخل أنبوب التصريف و تم وضع آخر عمودي يمثل ارتفاع أنبوب التصريف.تم تنفيذ الاختبارات للمحاكاة العددية باستخدام برنامج حزمة تحسيب حركة المائع المعروفة بال ANSYS FLUENT CFD و إتضح ان التشغيل عند التصريف الجزئي 50% الأكثر حده . ضخ الهواء عبر حوائط القمة المخروطيه لأنبوب التصريف قللت الدوامات عند 3 بار. و عند 5 بار تم توزيع ورفع الضغط المنخفض من 12.36% إلي اقل من 5% . وقورنت مع القيم عند التشغيل الأمثل , لذا يمكن استخدام الهواء للتقليل من نبضات الضغط وتكسير الدوامات لزيادة مساحة مخطط التشغيل في المحطة المائية بسد مروى.

Table of Contents

No	Description	Page
	Holy Quran (الآية)	i
	Dedication	ii
	Acknowledgments	iii
	Abstract	iv
	Abstract	v
	Tables of Contents	vi
	List of Tables	xii
	List of Figures	xiii
	List Symbols	xvi
	List Abbreviations	xvii

CHAPTER ONE: I

1.1	Introduction	2
1.2	problem Statement	2
1.3	Merowe Hydropower Plant	3
1.4	Objectives	4
1.5	Significances	4
1.6	Research Methodology	5
1.6 .1	Data Collection Merowe power plant	5
1.6 .2	Data Analysis	5

1.6 .3	Interpretation	5
1.7	Structure of the thesis	5

CHAPTER II: Literature Review and Theory

2.1	Introduction	8
2.2	Runner Outlet flow and Velocities	8
2.2.1	Best Efficiency operation	12
2.2.2	Full load operation	12
2.2.3	Part load operation	13
2.3	Draft Tube	13
2.3.1	Principles of operation of a draft tube	14
2.3.2	Pressure recovery	14
2.4	The swirl number	15
2.4.1	The Swirl Numbers a Function Of The Discharge And Speed Factors	15
2.5	Pressure Oscillation	17
2.6	Vortex Rope Frequency	18
2.7	Pressure pulsation	22
2.7.1	Pressure pulsation coefficients	23
2.7.1.1	The discharge coefficient ϕ and ψ energy coefficients	23
2.7.1.2	specific speed	23
2.7.1.3.	Thoma cavitation number	24
2.7.1.4	The Reynolds number Re	25

2.7.1.5	The Froude number Fr	25
2.8	Methods of reducing pressure pulsations	25
2.8.1	Air admission to the draft tube	26
2.8.2	water jet injection	30

CHAPTER III

Research Methodology & experimental

3.1	Introduction	33
3.1.1	Assumptions	33
3.2	Working of CFD code	33
3.2.1	Pre-Processing	34
3.2.2	Solver	34
3.2.3	ANSYS-FLUENT CFD Code	34
3.3	Draft Tube Geometry and domain	35
3.3.1	Geometry	35
3.3.2	Draft Tube domain	38
3.4	Runner	39
3.5	Flow Domain	41
3.5.1	Create named selections for the geometry boundaries.	41
3.6	Mesh Generation	41
3.6.1	Mesh Type and Topology	42
3.6.2	Mesh Quality	42

3.7	Grid sensitivity analysis	44
3.8	Boundary Condition Modeling	44
3.9	Inflow Plane	45
3.9.1	Runner Boundary conditions	46
3.9.2	Outflow Plane	47
3.9.3	Wall Boundary	48
3.9.4	Runner-Draft tube interface	49
3.10	Turbulence Model and transient simulations	49
3.10.1	Large eddy simulations (LES)	49
3.10.2	Advection scheme	50
3.10.3	Convergence criteria	50
3.11	Air admission simulations	50
3.12	Summary	52

CHAPTER IV

Results and Discussion

4.1	Introduction	54
4.2	Description of the M.D. Hydro power part load operation zone	54
4.3	Reynolds numbers, discharge coefficient (ϕ), Swirl number (S)	55
4.4	Draft Tube Flow Post-Processing	56
4.5	Numerical Prediction of Part Load Operation	56
4.5.1	Draft tube cross section contours	57

4.5.2	Draft tube Section at Operations at part load 70%, 60% and 50% Q_{BEP}	57
4.6	Air admission System 180°	58
4.6.1	pressure distribution at draft tube inlet horizontal section	58
4.6.2	pressure distribution at draft tube inlet vertical section	59
4.6.3	Vortex rope with the Q-criterion	60
4.6.4	Velocity streamlines plane with air admission System 180°	61
4.7	Air admission System 120°	62
4.7.1	Vortex rope with the Q-criterion	62
4.7.2	pressure distribution at draft tube inlet horizontal section	63
4.7.3	Draft tube vertical section with air admission System 120°	65
4.8	Discussion of Amplitude (ΔH) and pressure pulsations ($\Delta H/H\%$)	67
4.8.1	Air admission System 180°	67
4.8.2	Air admission System 120°	67
4.8.3	Hill chart modification	69
4.9	Comparison between two systems	69
4.10	Summary	70

CHAPTER V

Conclusion and Recommendation

5.1	Highlights	72
5.2	Conclusion	72
5.3	Recommendations for Future Studies	73

REFERENCES

References	75
------------	----

APPENDIXES

Appendix A: Merowe hill chart efficiency	79
Appendix B: Merowe hill chart rope zone	80

List of Tables

No.	Description	Page
Table 3.1	drafts tube dimensions	36
Table 3.2	Runner dimensions Characteristics	40
Table 3.3	Mass flow values for the operating points in fluent	45
Table 4.1	discharge description	54
Table 4.2	discharge coefficient	56
Table 4.3	Swirl number (S)	56
Table 4.4	The energy coefficient	56
Table 4.5	Amplitude (ΔH) and pressure pulsations ($\Delta H/H\%$)At $0.5Q_{BEp}$ partial load with air injection System 180°	67
Table 4.6	Amplitude (ΔH) and pressure pulsations ($\Delta H/H\%$)At $0.5Q_{BEp}$ partial load with air injection System 120°	68

List of Figures

Figure No.	Description	Page
Figure 2.1	Velocity triangles at the inlet and outlet of the runner	9
Figure 2.2	Velocity diagrams for a turbine runner	10
Figure 2.3	flow through a turbine	11
Figure 2.4	Velocity triangle for the outlet turbine at BEP	12
Figure 2.5	Velocity triangle for the outlet turbine at full load.	12
Figure 2.6	Velocity triangle for the outlet turbine at part load	13
Figure 2.7	runner outlet triangle by discharge condition	15
Figure 2.8	The change in the wicket gate momentum parameter $\Omega D/\rho Q^2$ with wicket gate opening angle.	20
Figure 2.9	Expected axial velocity profiles in the draft tube at different swirl numbers	21
Figure 2.10	Thomas variables	24
Figure 2.11	Schematic diagram of section and points for calculating pressure in the draft tube	26
Figure 2.12	Air admission path	27
Figure 2.13	Structure of air admission	28
Figure 2.14	Pressure fluctuation sat monitoring point p_1 at different Q_{air} .	28
Figure 2.15	Comparison of pressure contours between prototype (upper) and adding flow (lower)	29
Figure 2.16	Computational domain in a meridian half-plane for the test section with flow-feedback control system.	31

Figure 2.17	Schematic diagram of water replenishment	31
Figure 3.1	spiral case and draft tube	35
Figure 3.2	draft tube geometry	35
Figure 3.3	The draft tube and spiral case domain.	37
Figure 3.4	The draft tube and runner domains	37
Figure 3.5	The 3D draft tube geometry from the M.D. Hydro power plant	38
Figure 3.6	Draft tube cone accessory door	39
Figure 3.7	The draft tube (a) Top view	39
Figure 3.7	The draft tube (b) Side view	39
Figure 3.8	The M.D. hydro power model runner geometry in ANSYS	40
Figure 3.9	Mesh Quality	43
Figure 3.10	Body Sizing	44
Figure 3.11 (a)	smooth wall runner	47
Figure 3.11 (b)	inlet water boundary condition	47
Figure 3.12	outlet boundary condition	48
Figure 3.13	smooth wall boundary condition	48
Figure 3.14	Domain interface between runner and draft tube	49
Figure 3.15	data solution	50
Figure 3.16	Air injection path	51
Figure 4.1	M.D hydro plant operation zone	55
Figure 4.2	Pressure contour at the cross section of the draft tube at BEP	57
Figure 4.3	Operations at part load (a) 70% Q_{BEP} (b) 60% Q_{BEP} (c) and 50% Q_{BEP}	58
Figure 4.4	pressure distribution at draft tube inlet (cone section) section	58

Figure 4.5	Average pressure variation in the draft tube at cone operating condition; the pressure contours correspond to an instantaneous runner position at the end of unsteady simulation	59
Figure 4.6	Vortex rope with the Q-criterion	60
Figure 4.7	Velocity streamlines leaving the runner and across the cross section of the draft tube.	61
Figure 4.8	Vortex rope with the Q-criterion	62,63
Figure 4.9	pressure pulsations horizontal section	64,65
Figure 4.10	draft tube vertical section with stream lines	66
Figure 4.11	addional area on hill chart	69

List Symbols

Symbol	Definition	Unit
T	Time	[s]
Q	Discharge	[m ³ /s]
g	Gravitational constant	[m/s ²]
H	Head	[m]
C	Absolute velocity	[m/s]
u	Tangential velocity	[m/s]
w	Relative velocity	[m/s]
D	Diameter	[m]
r	Radius	[m]
M	Momentum	[Nm]
P	Power	[W]
E	Specific hydraulic energy [J/kg]	
A	Area	[m ²]
p	Pressure	[Pa]
U	Velocity	[m/s]

Greek letters

Symbol	Definition	Unit
ρ	Density	[kg/m ³]
ω	Angular velocity	[rad/s]
α	Guide vane angle	[°]
β	Flow angle	[°]
ε	Turbulent dissipation rate	[m ² /s ³]
κ	Turbulent kinetic energy	[m ² /s ²]
Ω	Turbulence frequency	[1/s]

List Abbreviations

3D	Three-Dimensional
BEP	Best Efficiency Point
DES	Detached Eddy Simulation
CFD	Computational Fluid Dynamics
HEXA	ANSYS ICEM CFD Hexa
HRS	High Resolution Scheme
LES	Large Eddy Simulations
VLES	Very Large Eddy Simulation
RM S	Root-Mean Square
rpm	Revolutions per minute
rps	Revolutions per second
FFT	Fast Fourier Transform
UDS	Upwind Difference Scheme
WGO	wicket gate opening

Chapter I

Introduction

Chapter I

Introduction

1.1 Introduction

A Francis turbine is one of the most commonly used in hydro power plants because of its wide range of operability(Wang, 2012). It uses the potential energy contained into a water head and transforms it into mechanical work by the use of a runner(Daqing, 2016). The water, stocked in a reservoir upstream, passes through the penstock and spiral case to put the runner in rotation(Gomes, 2017). The runner then drives the generator in rotation and electrical power is generated by induction between the generator stator and rotor. The flow finally leaves the turbine by the draft tube under the runner and returns to the river. Because of its reliability, high efficiency, and wide operating range, the Francis turbine is widely used in hydropower plants(ZUO, 2014).

The change consumption of energy results in hydro turbine plants operating at varying loads. Hydropower units must also operate reliably over a wide range of operating condition. So operating at off design (full and part load) undesirable operating can cause problems such as pressure pulsation ,vortex ,vibration and noise which may occur individually or in combination(Veli, 2013). Most of these problems are related to the transient behavior(Tørklep, 2012).According to the hydrology and the utilization strategy of a given hydraulic project. The nominal head and flow rate are determined for a power plant, then, depending on the number of machines and their rotational speed, which is related to the grid frequency and the number of poles in the generator, the type of hydro turbine can be chosen.

1.2 **problem Statement: -**

Francis turbine units will operate in part load discharge severe unsteady flow result of excessive swirl in the flow leaving the turbine runner occurring in the draft tube increase in pressure pulsation and vortex which in some cases may lead to unstable operation and greatest obstacles to be overcome in meeting this requirement is the problem of draft tube surging. (Müller, 2015)These pressure pulsation and vortex produce exciting forces that can affect components of the hydraulic, structural, mechanical, and electrical systems of a power plant.(Daqing, 2016)

The flow associated with draft tube pressure pulsation and vortex is classified as unsteady because the flow field within the draft tube varies with time; the discharge from the draft tube may or may not vary with time. The phenomenon is restricted to reaction type turbines, and is generally associated with units having fixed blades.(Fanelli, 2010)

As the absolute value of swirl in the draft tube increases, the axial velocity distribution in the draft tube becomes distorted. The flow becomes concentrated around the outside edge of the tube(Decaix , 2015). The onset of draft tube surging occurs when, at a critical level of swirl, the flow along the center line of the draft tube reverses, and a helical vortex forms around the periphery of the reverse flow region. The helix tends to rotate around the axis of the draft tube; this motion is described as the precession of the vortex. The formation of the helical vortex has been termed a vortex breakdown in the fluid mechanics literature(Harris, April 2013).

This thesis focusing on the numerical investigation of where air is injected in the Francis turbine draft tube cone wall flow in order to reduce the pressure pulsations and vortex phenomena's which occur when part load operation at low head. Water and air are the working fluids in these systems and even with consideration to their differences they have both been proven to produce positive results when operate at partial load in order to have already solved the operational range problem.

1.3 Merowe Hydropower Plant

Merowe power plant, built in 2008, is located close to the Merowe city north Sudan, and is part of a network of four hydro power plants at that time and others, taking advantage of the flow in the river Nile. The river is placed under strong regulatory laws and contract controlling flow of the river between Nile basin countries. The plant power capacity is 1250 MW divided over ten Francis turbines hydraulic turbine extracts energy at constant speed to supply the network at a given frequency (50 Hz). To guarantee that the runner speed does not change in time, a speed controller, named the governor, continuously monitors the runner speed. If for instance the runner starts accelerating, the governor gives the instruction to the distributor to close at a certain speed, characterized by the time it takes to close from a given opening.

1.4 Objectives: -

The overall objectives of this research presented in this project are physical understanding and Mitigation pressure pulsations ($\Delta H/H\%$) and breakdown the vortex rope formation in draft tube of the Merowe hydro power plant unit two at part load. In order to inject air in draft tube cone through cone wall unit two in Merowe hydropower plant at part load which severe pressure pulsation exist.

The purpose can be summarized in three principal objectives:

1. Evaluate the capabilities of ANSYS fluent to resolve and predict, three-dimensional, time-dependent flows (transient) vortex shedding.
2. Identify the physical location to optimize the positions of air injected in draft tube cone wall in order to injection air and mitigate pressure pulsations.
- 3- Determine the amount of air pressure to decrease the pressure pulsation and vortex rope through a hole in draft tube cone.

1.5 Significances: -

Due to the increased use of part-load operation, power companies assess the increased maintenance cost and risk of failure. At the present time, there is no way to accurately calculate these factors. Therefore, it is a desire to further study the pressure pulsation and vortex in Francis turbine outlet, to be able to increase flexible operation in part-load operation. However, the nature of these pulsation is not fully understood, even though they have been the topic of extensive research for two methods to inject air to the draft tube flow investigations can be chosen. The first one utilizes two portions (180°) in cone with specific geometry to inject air which provide clearly specified flow conditions of the draft tube. The second is three portions (120°) in the draft tube cone of the Francis turbine.

Finally, in addition to the direct environmental benefits of renewable energy, draft tube studies have indirect benefits: a better understanding of the flow characteristics within the draft tube allows better control of the mixing process in this component, e.g., for the air injection purposes, which is of prime importance for the local river life.

1.6 Research Methodology: -

The study is based on the information from the Merowe hydro power plant. The data are collected from the tiled experimental Merowe hydro power plant to analyze by numerical simulations computational fluid dynamic (CFD). Now day the computational fluid dynamic and relevant commercial software codes are well known are widely used for broad range of fluid flows applications. In this thesis both the commercial CFD software ANSYS Fluent and CFD code ICEM are used to analysis air injections.

1.6 .1 Data Collection Merowe power plant

Specification of Francis turbine considered under the present study take this operates parameters such as head, discharge, efficiency and output power are being recorded. This data has been acquired to be utilized to build and validate the simulation model.

1.6 .2 Data Analysis

The collected data have been used to build a computational model which is used to predict the pressure pulsations and vortex at different part load operating conditions

1.6 .3 Interpretation

Collected data and that obtained from the simulation are compared to the published literature and ALSTOM Guaranteed value at operation zone

1.7 Structure of The Thesis

The thesis is dealing with one major topic within flow fields in draft tube Francis turbines at part load and is presented as follows:

In Chapter 2, the literature of pressure pulsation and the history of draft numerical mode, the methods which govern the pressure pulsations developments in Francis turbine draft tube are discussed. Finally, the different conditions in which a Francis turbine operates are described in details along with the state of art in the simulation of these conditions.

In Chapter 3, transient events in hydraulic turbines are the subject of interest. First, the introduction of heart in the simulation of transient events is presented in details. Moreover, relevant assumptions are established to perform reliable, numerical simulations during the part load. The mixture simulation characteristics by a three-dimensional method

are also treated. Finally, the flow topology during the part load is predicted with a numerical approach combined to field data observations. Two air injection approaches available in the chosen numerical solver are assessed and the physical mechanisms resulting from the simulations are discussed.

The relevant phenomena of pressure pulsations vortex are described in details in Chapter 4. First, two sections regimes and patterns of pressure pulsations and vortex rope in Francis turbines draft tube are discussed. The physical behaviors of this water air mixture are also considered to a great extent. Then, the matter of numerically representing contours and streamline are presented in commercial solvers such as ANSYS post process are discussed. Finally, simulations are performed to identify if pressure pulsations and vortex rope are phenomenon's sensitive.

Finally, the thesis ends with a proper conclusion and openings toward future works in Chapter 5.

CHAPTER II

Literature Review

And Theory

CHAPTER II

Literature Review

And Theory

2.1 Introduction

Most Francis turbines are prone to vortex rope when operating off design conditions (or operate out the best efficiency point (BEP)) at partial load ($Q < Q_{BEP}$) or overload conditions where the flow rate ($Q > Q_{BEP}$) (Ciocan, 2007). The complex unsteady flow developing in the draft tube of a Francis turbine at part load is responsible for pressure pulsation, which could prevent the whole hydro power plant from operating safely (WANG, 2015). Indeed, the Francis draft tube cone is subjected to inlet swirling flow, the swirling flow injected by the constant pitch turbine runner in the draft tube yields to the development of a helical vortex core rotating in the draft and operation in a narrow range close to the optimal conditions. (Foroutan, 2015)

Swirling flows are characterized by simultaneous axial and rotation motion. The change in the flow pattern, from steady state symmetric flow to unsteady helical flow, when angular momentum is increased, is named as the vortex breakdown phenomenon (as a result of the mismatch between the swirl generated by the guide vanes and the angular momentum extracted by the turbine). (Tridon, 2010)

2.2 Runner Outlet Flow and Velocities

The velocity exiting in the runner depends on the operating conditions of the turbine as shown in figure (2.1). Because in Francis turbines blade angle β is fixed, the relative angle between U the blade velocity and W relative velocity at the runner outlet is practically constant for every operating point. Where C_m and C_t are the axial (or meridional) and tangential velocity at the outlet of the runner and inlet to draft tube. They are presented in figure 2.1 (Daqing, 2016), and C is the absolute velocity. Also the flow through wicket gate and guide vane in figure 2.2 and figure 2.3. (KIRSCHNER, 2007)

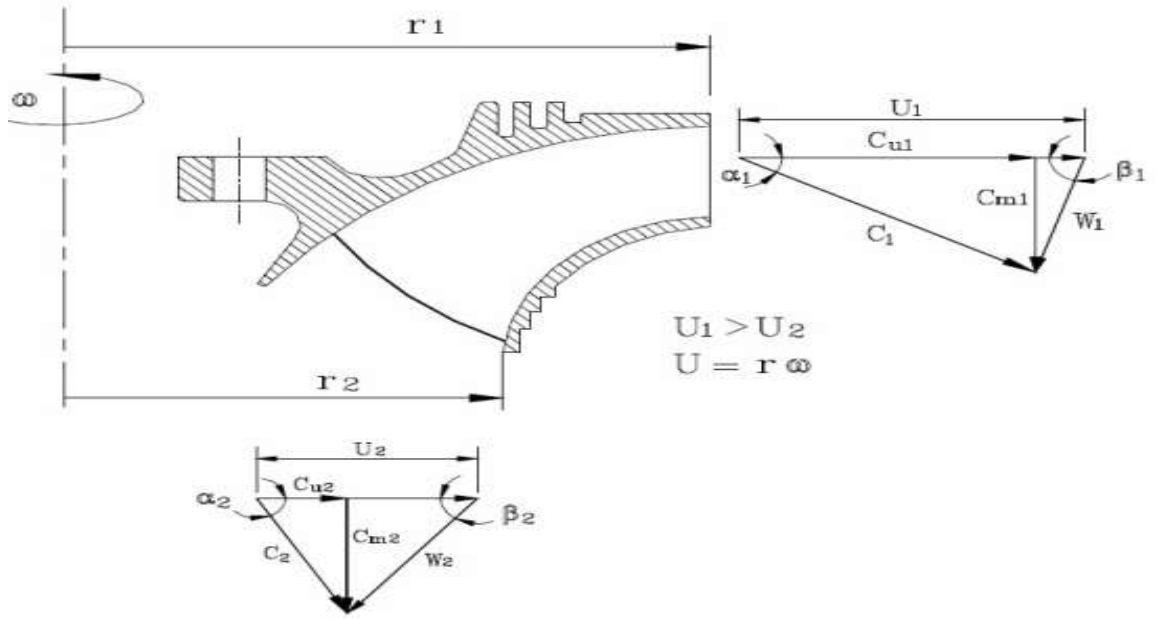


Figure 2.1 Velocity triangles at the inlet and outlet of the runner (KIRSCHNER, 2007)

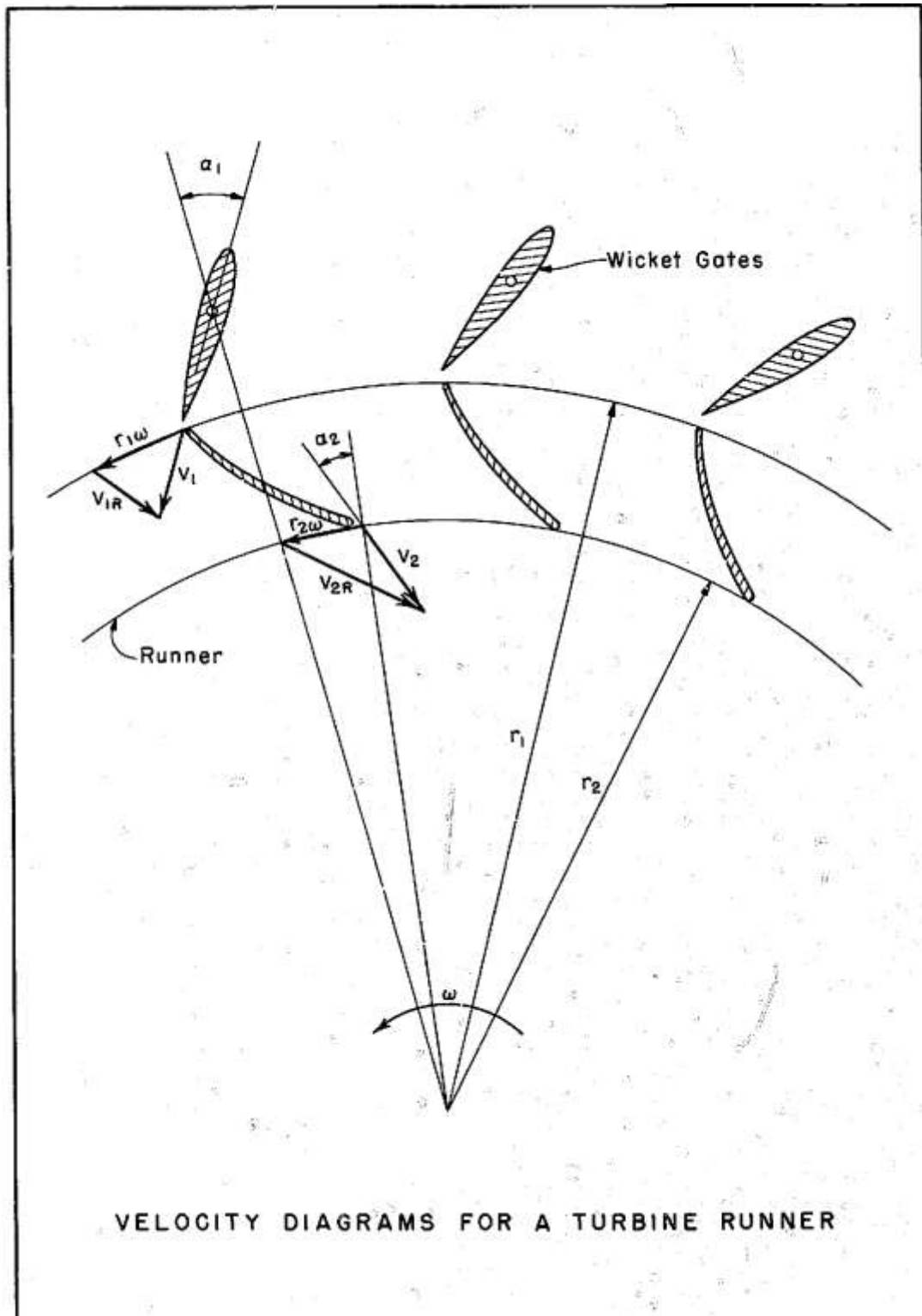


Figure 2.2 Velocity diagrams for a turbine runner(FANELLI, 2010).

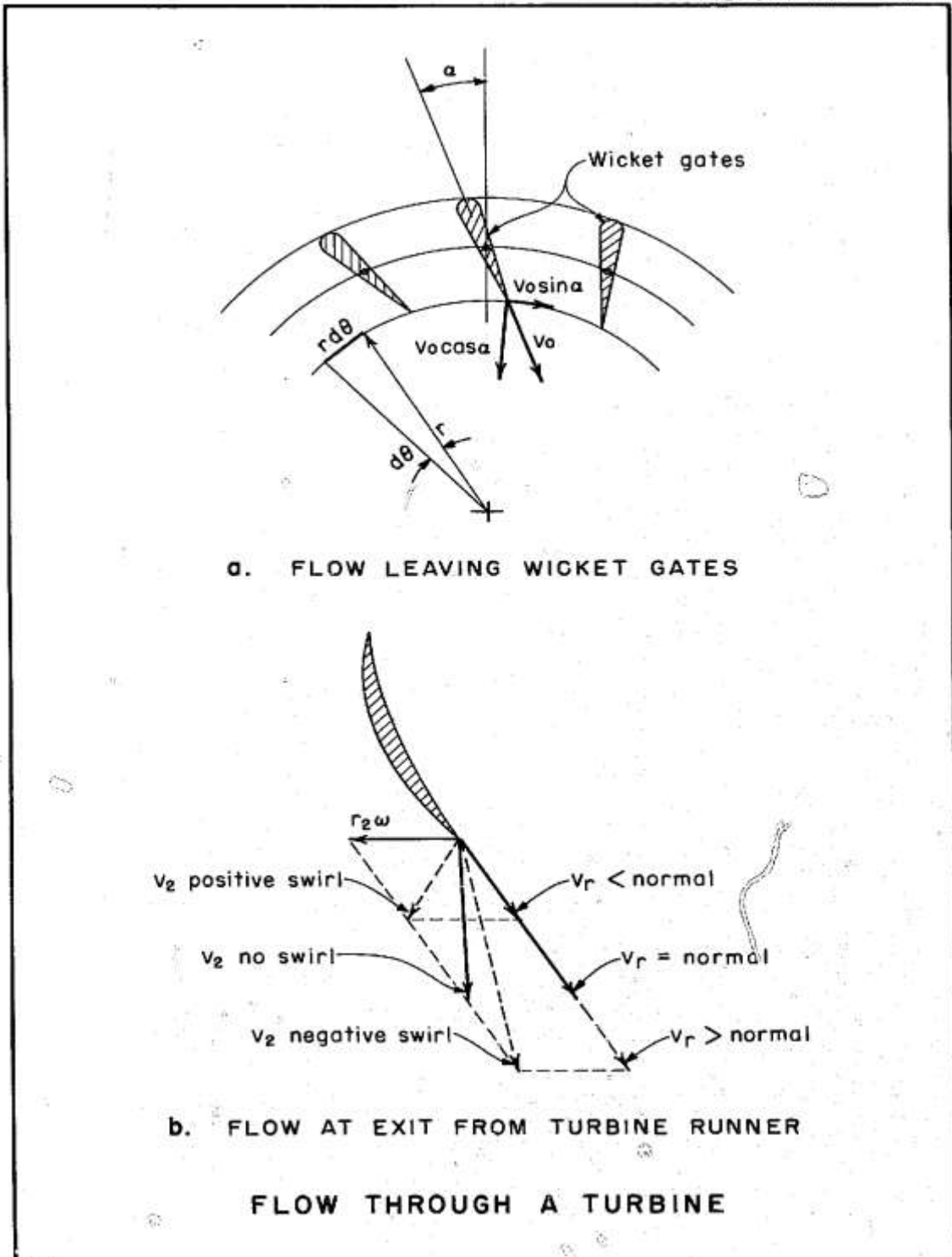


Figure 2.3 flow through a turbine(FANELLI, 2010).

2.2.1 Best Efficiency Operation

At the best efficiency point (BEP) the flow leaving the runner and ingested by the draft tube is close to purely axial has little or no rotation(KRANE, 2015). In theory, C_{2u} is zero, where ($C_t = 0$ and $C = C_a$).see Figure (2.4)(Nicolet, July 2, 2004) shows the outlet velocity triangle at the BEP. However, in practice, to prevent flow separation from the draft tube wall and to minimize hydraulic losses associated with kinetic energy-to-static pressure conversion in the draft tube, a certain level of residual swirl is provided at the runner outlet(Arthur Favrel, 2017). This swirling flow at the draft tube inlet is tuned for optimal performance at the best efficiency operating (Viktor Iliev, 2012)point.

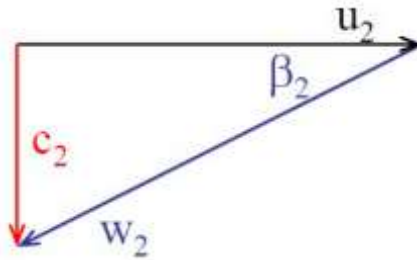


Figure 2.4 Velocity triangle for the outlet turbine at BEP(Viktor Iliev, 2012).

2.2.2 Full Load Operation

At full load, the runner is unable to utilize all the rotation in the flow, the flow leaving the runner has a reduced rotation in the same direction as the flow entering the runner. Figure 2.5(Nicolet, 2004) the flow entering the draft tube is rotating in the opposite direction of the runner(Doerfler, 2016).

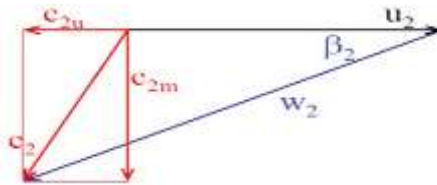


Figure 2.5 Velocity triangle for the outlet turbine at full load(Viktor Iliev, 2012).

2.2.3 Part load Operation

At part load the rotation in the flow is reversed, the flow entering the draft tube rotates in the same direction as the runner. Figure 2.6(Nicolet, July 2, 2004) shows the outlet velocity triangle for a runner at part load.

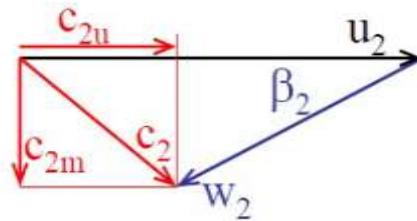


Figure 2.6 Velocity triangle for the outlet turbine at part load(Viktor Iliev, 2012).

(U_2 is the runner velocity, W is the relative velocity, and C_2 is the absolute velocity leaving the runner and ingested by the draft tube, with C_a and (C_{2u}) C_t being axial and circumferential (swirl) components.)

2.3 Draft Tube

Draft tube is an important part of reaction turbine (Francis turbine) which serves the following purposes:

- Used to convert kinetic into static pressure available at outlet of runner into pressure head, thereby, increasing the overall output(Brunes, December 2009).
- To install the turbine runner above or below the tail water level to avoid cavitation's, without affecting the net head.

Different types of draft tubes and specifications.

- Straight conical draft tubes.
- Bell mouth draft tubes.
- Elbow draft tubes.

The cross section of the draft tube inlet is circular, bent at an elbow. Then the cross section become elliptic and later rectangular at diffuser with rounded corners.

2.3.1 Principles of Operation of a Draft Tube

The principle of a draft tube can be outlined by applying Bernoulli's equation across the draft tube as shown in Equation (2.1).

$$\frac{P_1}{\rho g} = \frac{P_{atm}}{\rho g} - \left\{ H_s + \left(\frac{\alpha_1 V_1^2}{2g} - \frac{\alpha_2 V_2^2}{2g} - h_f \right) \right\} \quad 2.1$$

Where p_{atm} is the atmospheric pressure, P_1 is pressure at the inlet of the draft tube, H_s is the turbine installation height (suction head) assumed as approximately equal to z_1 , h_f is the head loss, V_1 and V_2 are the velocities at the inlet and outlet of the draft tube, respectively, α_1 and α_2 are the velocity correction factors at the inlet and outlet of the draft tube, respectively, ρ is the density of the liquid and g is the acceleration due to gravity. From Equation (2.1) it can be seen that a draft tube generates a low pressure region below the runner, which can be utilized by the turbine. This lower pressure consists of two terms; static pressure drop (H_s) and dynamic pressure drop $\left(\left(\alpha_1 V_1^2 / 2g \right) - \left(\alpha_2 V_2^2 / 2g \right) - h_f \right)$. H_s is independent of the discharge while dynamic pressure drop is discharge dependent. This dynamic pressure drop increases by increase in diffuser wall angle and/or by enlarging the draft tube length. In both cases, however, the hydraulic losses will become larger. An efficient draft tube has the reform an optimal diffuser angle and length for which the pressure reduction below the runner will be maximal. (Helmrich, 2015.)

2.3.2 Pressure Recovery

In practice, the hydraulic performance of a draft tube is quantified by the pressure recovery coefficient given by the following equation. (Ruchonnet, 2012)

$$x = \frac{\left(\frac{P}{\rho} + gz \right)_{outlet} - \left(\frac{P}{\rho} + gz \right)_{inlet}}{\frac{Q_2}{2A_{inlet}^2} \left[1 - \left(\frac{A_{inlet}}{A_{outlet}} \right)^2 \right]} \quad 2.2$$

The numerator in Eq.2.2 Is the difference in potential energy and the denominator is the difference in kinetic energy from inlet to outlet of the draft tube. For an ideal draft tube with no losses the pressure recovery factor is equal to one. However, in practice, losses including friction, flow separation, and flow blockage result in lower pressure recoveries. Most of the pressure recovery occurs in the draft tube inlet cone (Breivik, 2011).

2.4 The Swirl Number

Experience has shown that the main factor for triggering the vortex breakdown is the dimensionless swirl number is used to describe the amount of swirl present in the flow is the so called swirl number (S), is defined as the ratio of angular flux of moment-of-momentum to the axial flux of axial momentum times the inlet radius (Nishi, 2015).

$$S = \frac{\text{Angular momentum}}{\text{Axial momentum}} \quad 2.3$$

$$S = \frac{\int v_{ax} v_{tan} r ds}{R \int v_{ax}^2 ds} \quad 2.4$$

An increase in the swirling velocity component will result in increased axial velocity around the draft tube edges and a reduction in axial velocity at the center of the tube (Kuibin, 2010). In swirling flows the velocity relative to the surrounding fluid can become very high and if recirculation starts to occur in the central region of the flow, the water at the boundaries of this region experiences very large differences in relative velocity which results in a drastic decrease in pressure (Gavrilov, 2016).

2.4.1. The Swirl Numbers a Function of the Discharge and Speed Factors.

$$n_{ED} = \frac{nD}{\sqrt{E}}, \quad Q_{ED} = \frac{Q}{D^2 \sqrt{E}}$$

The swirl number as a function of the operating parameters is derived by Rudolf and considering the velocity diagrams and a simple representation of the flow at the runner outlet. Figure 2.7 runner outlet triangle by discharge condition. (Nicolet1, 2009)

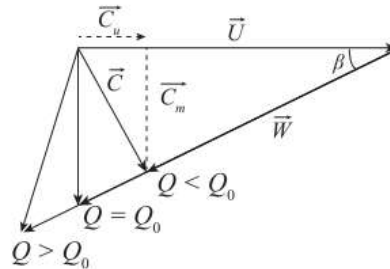


Figure 2.7 runner outlet triangle by discharge condition. (Nicolet1, 2009)

For a given value of the runner frequency, i.e. for a given n_{ED} -value, there is a value of discharge Q_{BEP} for which the flow at the runner outlet is theoretically axial. In such conditions, called swirl-free conditions in the following, the relative flow angle β at a given radial position r can be expressed as follows:

$$\tan\beta = \frac{v_{a.BEP}}{U} = \frac{v_{a.BEP}}{\omega r} \quad 2.5$$

where $V_{a.BEP}$ is the axial flow velocity corresponding to the discharge Q_{BEP} , U is the runner circumferential velocity and ω is the angular speed of the runner.

When the discharge is decreased below the value Q_{BEP} , the machine operates in part load conditions and a tangential flow velocity component V_u appears at the runner outlet, as illustrated in Fig. 2.7. At these conditions, V_u can be expressed for a given radial position r as a function of the axial velocity component V_a and the angular speed of the runner ω : (Pavel Rudolf, 2010)

$$\tan\beta = \frac{v_a}{U - V_u} = \frac{v_a}{\omega r - V_u} = \text{constant} = \frac{v_{a.BEP}}{\omega r} \quad 2.6$$

The below expression is, then, introduced in the definition of the swirl number. By considering that the axial flow velocity is independent of the radial position,

i.e. $V_a = 4Q / \pi D^2$, and the angular speed of the runner ω :

$$S = \frac{\int_0^R V_a \cdot \omega \cdot r \cdot \left(1 - \left(\frac{V_a}{v_{a.BEP}}\right)\right) \cdot r^2 \cdot dr}{R \int_0^R V_a^2 \cdot r \cdot dr} \quad 2.8$$

$$S = \frac{\omega}{R} \left(\frac{1}{V_a} - \frac{1}{v_{a.BEP}} \right) \cdot \frac{\int_0^R r^3 \cdot dr}{\int_0^R r \cdot dr} \quad 2.9$$

$$S = \frac{\omega \cdot R}{2} \left(\frac{1}{V_a} - \frac{1}{v_{a.BEP}} \right) \quad 2.10$$

The axial flow velocity is expressed as a function of the discharge Q and the speed and discharge factors are introduced in Eq. (10). The following expression for the swirl number is finally obtained:

$$S = n_{ED} \frac{\pi^2}{8} \cdot \left(\frac{1}{Q_{ED}} - \frac{1}{Q_{ED,BEP}} \right) \quad 2.11$$

where $Q_{ED,BEP}$ is the discharge factor in swirl-free conditions for a given speed factor.

2.5 Pressure Oscillation

Pressure oscillation may occur in many different parts of a system and many sources of oscillations. The most common low-frequency pressure oscillation for a hydropower system is caused by the draft tube vortex (IEC, 1999). In 1940 W. J. Rheingans found that oscillations in vacuum or pressure in the draft tube (Rheingans frequency) caused oscillations in the effective head which again caused oscillations in the power efficiency (Rheingans, 1940). From rotational effects it is typically four pressure oscillations which cause significantly high amplitudes (ALLIGNÉ, 2011)

1- runner frequency

The runner frequency can give powerful impulses if the runner vanes are damaged, the runner is unbalanced or if the flow is unsymmetrical (Fay1, 2010).

$$f_n = \frac{n}{60} \text{ [Hz]} \quad 2.12$$

2-runner vane frequency

This frequency is an oscillation which occurs every time a runner vane passes the same guide vane. The amplitude from this oscillation is the dominating amplitude under stable operational conditions. The amplitude will also be influenced by the distance between the impeller and the guide vanes and therefore by guide vane opening

$$f_b = f_n * z_b \text{ [Hz]} \quad 2.13$$

3-Guide vane frequency

The guide vane frequency is caused by an impulse given by damage on the runner. The impulse will occur every time the damaged part passes a guide vane.

$$f_g = f_n * z_g \text{ [Hz]} \quad 2.14$$

4-Rheingans frequency

The cause of Reagans, or draft tube vortex frequency, is a mass fluctuation which occurs in the draft tube. The amplitude of the Reagans frequency gets predominant only when the vortex is visible to the naked eye. This means when the pressure becomes so low that the vortex is filled with air(Zhong-dong , 2007).

$$f_R = f_n / 3.6 [\text{Hz}] \quad 2.15$$

2.6 Vortex Rope Frequency

At large Reynolds numbers (typical in hydro applications) the viscous effects are negligible. Therefore, it can be assumed that the frequency is independent of the Reynolds number. Therefore, for a given draft tube with a fixed geometry (i.e., $L/D = \text{const.}$) the frequency of the vortex rope is a function of only the swirl number, i.e.,(Constantin TĂNASĂ,2011)

$$\frac{fD^3}{Q} = g\left(\frac{\Omega D}{\rho Q^2}\right) = g(s) \quad 2.16$$

The exact form of the function g is obtainable by performing extensive experiments for; several inlet swirl numbers. It should be noted that g is unique for a specific draft tube shape(J.Plade, July 1972).

In order to obtain a relation for the vortex rope-to-runner frequency ratio, the flow rate in the left-hand side of Eq. (2.16) is replaced by the discharge coefficient using Eq. (2.17). Furthermore, considering $R = D/2$ being the draft tube inlet radius (equal to the runner outlet radius) and $\omega = 2\pi f_n$ being the runner angular velocity, Eq. (2.16) can be written as

$$\frac{f_v}{f_n} = \frac{\pi^2}{4} \varphi g(s) \quad 2.17$$

Hydro turbine typically has a constant head and rotational speed, and the flow rate is adjusted by the wicket gate opening which defines the operating point of the machine. Therefore, for a typical Francis turbine with a known head and rotational speed, the right-hand side of Eq. (2.17) is a function of only the wicket gate opening (WGO). Wicket gates add an angular momentum Ω_0 to the flow, part of which is extracted by the runner as the

torque Therefore the angular momentum of the flow leaving the runner and entering the draft tube is

$$\Omega = \Omega_0 - T = \Omega_0 - \frac{P}{\omega} \quad 2.18$$

where $P = \eta\rho gH$ is the runner mechanical power and

$\omega =$ is the angular velocity of the runner.

The dimensionless angular momentum parameter (the swirl number) can be written as

$$s = \frac{\Omega D}{\rho Q^2} \quad 2.19$$

$$= \frac{\Omega_0 D}{\rho Q^2} - \frac{PD}{\rho Q^2 \omega} \quad 2.20$$

The first term on the right-hand side of Eq. (2.20) is called the wicket gate momentum parameter ($\frac{\Omega_0 D}{\rho Q^2}$) and can be related directly to the WGO. For example, it is shown that

$$\frac{\Omega_0 D}{\rho Q^2} = 59 (\text{WGO})^{-1.18} \quad 2.21$$

Where WGO is the opening angle of the wicket gates in degrees, measured from 0 when fully closed. Figure (2.8) shows the value of the wicket gate momentum parameter as a function of the gate opening.

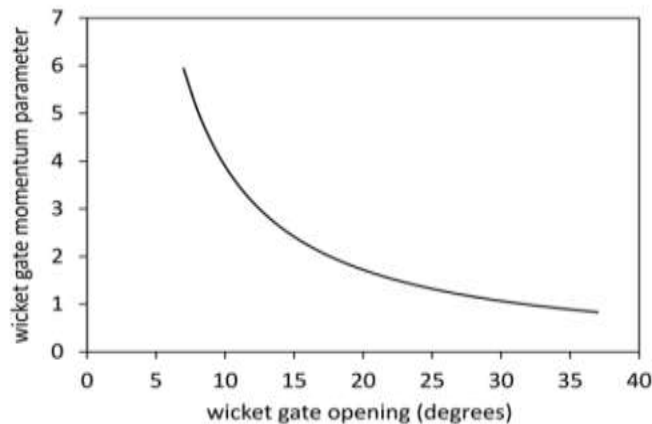


Figure 2.8 The change in the wicket gate momentum parameter $\Omega D/\rho Q^2$ with wicket gate opening angle (Constantin TĂNASĂ, 2011).

The second term on the right-hand side of Eq. (2.22) is the swirl extracted from the flow by the turbine runner Using head and flow rate coefficients.

$$\frac{PD}{\rho Q^2 \omega} = \frac{1}{\pi} \left(\frac{\psi}{\phi} \right) \quad 2.22$$

By substituting Eq. (2.21) and (2.22) in Eq. (2.17), another form for the vortex rope-to-runner frequency ratio is obtained

$$\frac{f_v}{f_n} = \frac{\pi^2}{4} \phi g \left[h(\text{WGO}) - \frac{1}{\pi} \left(\frac{\psi}{\phi} \right) \right] \quad 2.23$$

where h is some function of WGO, for example, the right-hand side of Eq. (2.23). This form clearly shows that the ratio between the frequencies of the vortex rope and the runner is a function of only the WGO which defines the flow rate coefficient ϕ for a specific machine with fixed head ψ and rotational speed ω .

The simplest choice for the function g is a constant. This is inspired by the experimental measurements of Wahl in a model (1:40) test of the 700 MW turbine installed at the Grand Coulee third power plant. As shown in Fig. 2.11, the frequency parameter is almost constant for swirl numbers less than one (remember that the swirl number in the FLINDT draft tube for case D with 70% of the BEP flow rate was 0.63.). Figure 2.11 suggests the value of 0.5 for the frequency parameter, i.e., (Ciocan, 2007)

$$\frac{fD^3}{Q} = 0.5 \quad 2.24$$

Hence, using Eq. (2.17), the relation for the vortex rope frequency is found to be

$$\frac{f_v}{f_n} = \frac{\pi^2}{8} \phi \quad 2.25$$

In the case of the FLINDT draft tube, for the operating point D with $\phi = 0.26$, Eq. (2.29) gives the value of $f_v/f_n = 0.32$ which is in close agreement with the experimental value of

0.3. Furthermore, the linear increase of the vortex rope frequency with the discharge coefficient (suggested by Eq. (2.25)) is shown in Figure 2.9 Expected axial velocity profiles in the draft tube at different swirl.

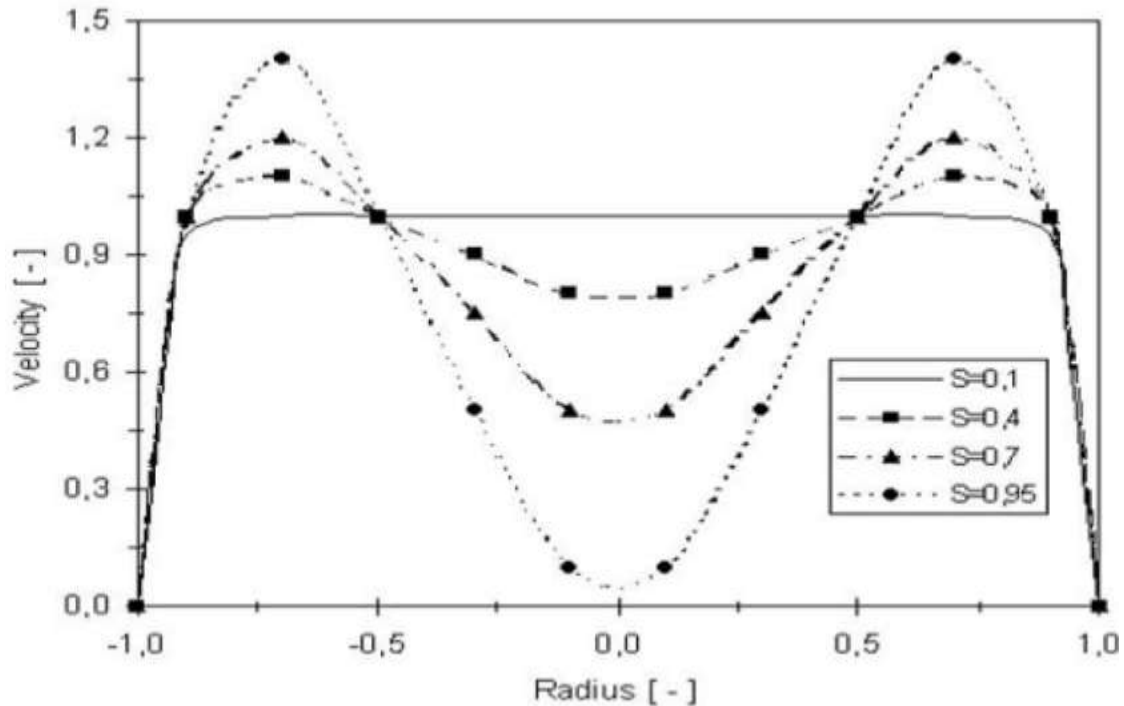


Figure 2.9 Axial velocity profiles in the draft tube at different swirl(J.Plade, July 1972).

2.7 Pressure Pulsation

When the flow downstream the runner at BEP, it does not have a tangential velocity (no swirl), significance the flow is perpendicular to the shaft axis. At operation partial load, the direction of the exit flow changes and generate a tangential velocity component. The pressure internal the vortex is lower than the pressure in the surroundings, with generate pulsations every time the vortex passes a specific point on the wall. The amplitude becomes dominant at part load, as the rope swings approaching to the draft tube wall, amplifying the oscillations(Susan-Resiga, 2006).

A lot of research has been performed by many scientific branches among the first major works presented on dynamic instabilities was “Power swings in hydroelectric plants”, published in 1940 by W. J. Rheingans .The investigation is undertaken for

operating conditions corresponding to low discharge, i.e., 0.65–0.85 times the design discharge, which exhibits pressure pulsation at surprisingly high frequency value, between 2 and 4 times the runner rotation frequency.

PhD student Einar Korbo studied pressure pulsations in Francis turbines, Significant part of his research was to establish the connection between the pressure pulsations in Francis model and prototype runners, with main focus on steady state. operations (Kobro, 2010).

Kirschner, a research team from China an experimental investigation of pressure pulsations and vibration in a large Francis turbine. They performed measurements at the Three-gorges hydropower Plant in China, investigating vibrations at unsteady flows(Kirschner, 2012). This research concluded that reducing the pressure pulsation intensity would also reduce the vibrations in the system. “Flow induced pulsation and Vibration in Hydroelectric Machinery” by Dörfler, Sick and Coutu (2006), has been used extensively in addition to the publications.

2.7.1 Pressure Pulsation Coefficients

2.7.1.1 The discharge Coefficient (ϕ) and (ψ) Energy Coefficients

Since operation is usually done at a known constant runner speed, it is convenient for hydraulic performance purposes to use dimensionless coefficients for the discharge and net head. Both these coefficients were introduced by the dimensionless Navier-Stokes

First, a discharge coefficient ϕ is proposed in the form of

$$\phi = \frac{C_m}{U} = \frac{4Q}{nD^3\pi^2} = \frac{Q}{\pi\omega R^3} \quad 2.26$$

ϕ^* specific discharge coefficient divided by the ϕ BEP value ($\phi^* = \phi / \phi_{BEP}$)

Secondly, an ψ specific energy coefficient or pressure parameter is expressed as:

$$\psi = \frac{2gHn}{U^2} = \frac{2gHn}{(\pi nD)^2} = \frac{2gH}{\omega^2 R^2} \quad 2.27$$

ψ^* specific energy coefficient divided by the ψ BEP value ($\psi^* = \psi / \psi_{BEP}$)

The dimensionless coefficients of the head ψ and of the flow rate ϕ allow comparison with other machines of different dimensions and rotational speeds and are defined .Here H is the turbine head, Q is the turbine flow rate, ω is the runner angular velocity, and R is the runner radius.

2.7.1.2 Specific Speed

The intensive investigations of draft tube pressure pulsations on various specific speed turbines were performed in 1990's and the results are published in to. Tests were performed in the wide turbine operating range from partial to full load and from runaway to head above optimum. The specific speed of the machine is defined as follows

$$v_s = \omega \frac{(Q/\pi)^{1/2}}{(2gH)^{3/4}} = \frac{\phi^{1/2}}{\psi^{3/4}} \quad 2.28$$

Usually, those pressure pulsation , featuring significant amplitudes, are found on the Francis turbine scale model of high specific speed, $v_s > 0.45$, and for low σ values.

Depending on the specific speed, Francis turbines are divided into three types: low- ($v_s \leq 0.35$), medium-, and high-speed ($v_s \geq 0.6$). For high specific speed machines the draft tube is the most critical component with respect to losses.

2.7.1.3. Thomas Cavitation's Number

If cavitation's occurs in the flow, in other words: if the gaseous phase partly replaces the liquid phase of fluid, then the absolute pressure level plays an important role. The most common variable is the Thomas cavitation number. The term in brackets is also called NPSH (,Net Positive Suction Head ') H_B therein is the barometric head, in meters of water column, and H_S the elevation of a typical reference point of the machine above a (virtual or real) free water surface with barometric head H_B , while H_V is the vapor (saturation) pressure pertaining to the actual water temperature. For the reference elevation for H_S the center of the wicket gate is often selected.

$$\sigma = (H_B - H_S - H_V) / H \quad 2.29$$

$$\sigma = \text{NPSH} / E \quad 2.30$$

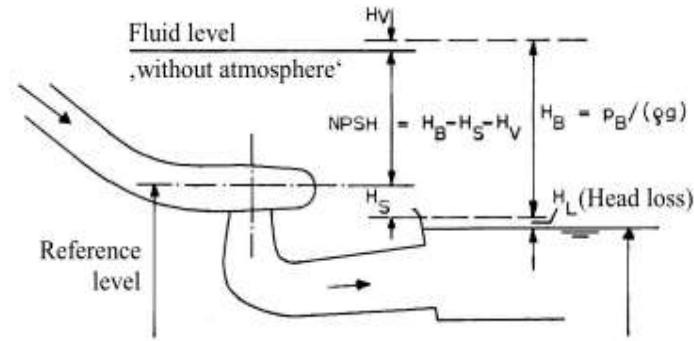


Figure 2.10 Thomas variables

It can be noticed, that the frequency of the vortex precession slightly decreases from 0.4 to 0.31fn when σ is increased and the related amplitude is rather constant, except for $\sigma < 0.45$, where amplitudes are reduced by a factor of 2. This is similar to the observations already made by Jacob.

More interesting is the impedance of σ on the frequency and amplitude of the pressure pulsation in the range of 2–4 f_n . The fundamental frequency value of these pressure pulsation is Quasi proportional to the Thoma cavitation number, while the amplitudes strongly increase when σ is below 0.45.

2.7.1.4 The Reynolds Number (Re)

The dimensionless parameter resulting from the momentum equation is the ratio of viscous forces on inertial forces, which can also be expressed by the Reynolds number Re. The definition of the Reynolds number applied to the runner by hydraulic engineers usually involves the tip speed U in the form expressed by the right of equation

$$Re = \frac{UD}{\nu} = \frac{\pi n D^2}{60\nu} \quad 2.31$$

In the stability analysis of a fluid flow, the Reynolds number can be indicative of the state of the flow from laminar to turbulent. The typical order of magnitude of the Reynolds number in a hydraulic turbine ranges from 10^5 to 10^8 , respectively from reduced geometries to installed prototypes. However, without that range, the flow is always considered fully turbulent.

2.7.1.5 The Froude Number (Fr)

The dimensionless form of the Navier-Stokes equation also allows to identify a ratio of the gravitational and inertial forces in the form of the Froude's number:

$$F_r = \frac{U^2}{gD} \quad 2.32$$

2.8 Methods of Reducing Pressure Pulsations

The methods distinguish between active and passive installations. Active installations distinguish themselves from passive installations because they require something to be continuously added to the system. Typical active installations use water and air injections (C TANASA1, 2016). These are often injected either through the hub of the turbine or through the wall of the draft tube. Air injection will change the viscosity of the water in the draft tube. Passive installations have the advantage that when they first have been installed, they are considered permanent and do not need any additional control system to alter them. Traditionally the development has focused on fins in the draft tube and runner cone extensions (C TANASA1, 2016).

2.8.1 Air Supply to the Draft Tube

In general, the air supplies to draft tube cone from different situations to eliminate or reduce pressure pulsation. (Air will flow to the low pressure zones in the flow) and results

QIAN Zhong the computational results show: air admission from spindle hole decreases the pressure difference in the horizontal section of draft tube, which in turn decreases the amplitude of low-frequency pressure pulsation in the draft tube; show the Fig.11 Schematic diagram of section and points for calculating pressure in the draft tube (Zhong-dong, 2007).

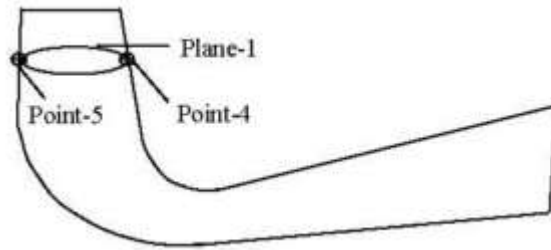


Fig.11 Schematic diagram of section and points for calculating(Zhong-dong, 2007).

pressure in the draft tube

- Renfang Huang numerical simulation of pressure vibration in Francis turbine draft tube with air admission through crown holes and spindle hole has been tested. The results indicate the pressure vibrations in the turbine are reasonably predicted by the present numerical method Figure 12 Air admission path (Huang, 2014).

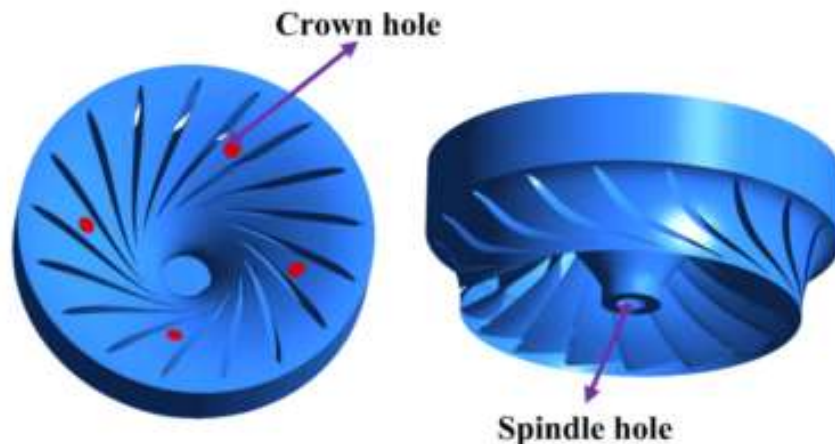


Figure 12 Air admission path(Huang, 2014).

Xianwu Luo The results show that aeration with suitable air flow rate can alleviate the pressure fluctuations in the draft tube, and the mechanism improving the flow stability in the draft tube is due to the change of vortex rope structure and distribution by aeration, i.e. a helical vortex rope at a small aeration volume while a cylindrical vortex rope with a large amount of aeration. The preferable vortex rope distribution can suppress the swirl at the smaller flow rates, and is helpful to alleviate the pressure fluctuation in the draft

tube. The analysis based on the vorticity transport equation indicates that the vortex has strong stretching and dilation in the vortex rope evolution(Xianwu Luo1, 2017).

- Yunheung Jeon study Effect of Air Admission on Pressure Pulsation in a Francis Turbine he conclude Air was admitted through the cone and pressure pulsation gradually decreased with increase of air flow and kept nearly constant after 5% of the rated flow(Jeon, .2014).

- Veli The problem is the station has a direct negative effect on the alternator capacity, was solved by adding an air-admission system. In doing so, power production was increased by 11.11%, from 44 MW to 49.5 MW. This caused a significant head loss, specifically in the Francis turbines. Vortex optimization was successfully established at the Darca-1 HPP. Fig.2.13 Structure of air admission (Veli, 2013).

The dominating frequency is decided by the runner frequency, the shape of the runner and the draft tube and cannot be changed by air admission. With air admission, the pressure difference in the section of draft tube decreases, while the amplitude of pressure pulsation decreases when increase the air

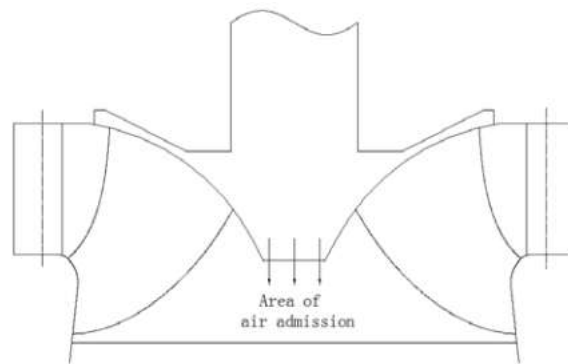


Fig.2.13 Structure of air admission(Veli, 2013).

-A Yu, X W Luoand B Ji 's and her “Numerical simulation, air admission from the main shaft center is applied, the analysis based on the vorticity transport equation shows that the vortex dilation plays a major role in the vortex evolution with air admission in the turbine draft tube, and there is large value of vortex dilation along the vortex rope. The results show that the aeration with suitable air volume fraction can depress the vertical

flow, and alleviate the pressure pulsation in the draft tube Pressure fluctuation at monitoring point p_1 at different

Q_{air} (A Yu1, 2015).

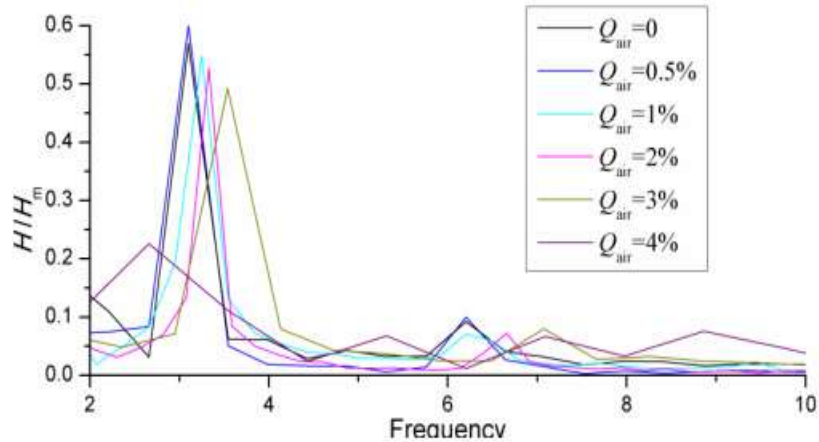


Figure 2.14 Pressure fluctuation sat monitoring point p_1 at different Q_{air} (A Yu1, 2015).

S. G. Scripting, The Effect of Air Injection on the Parameters of Swirling Flow in a Turbine99 Draft Tube Model, Gas injection leads to a change in the frequency of precession of the vortex core formed in the draft tube cone, which is not related to an increase in the gas–liquid mixture flow rate (S. G. Skripkina, , 2014)

The air flow rate (Q_{air}) is calculated as shown in equation (2.33), where φ represents the imposed rate for the injected air, and Q_{water} is the water flow rate.

$$Q_{air} = \frac{\varphi Q_{water}}{100} \quad 2.33$$

In order to produce the optimal effect air injection, the proper amount of air has to be determined. The recommended amount of injected air varies between 0.06% to 4% of the water flow rate.

Adding air to the draft tube can reduce the amplitude of pressure fluctuation caused by the vortex rope in the draft tube but cannot change the main frequency of the pressure fluctuation, failing in solving the problem of high fluctuation of output power of the turbine Fig.2.14 (W F Li, 2015).

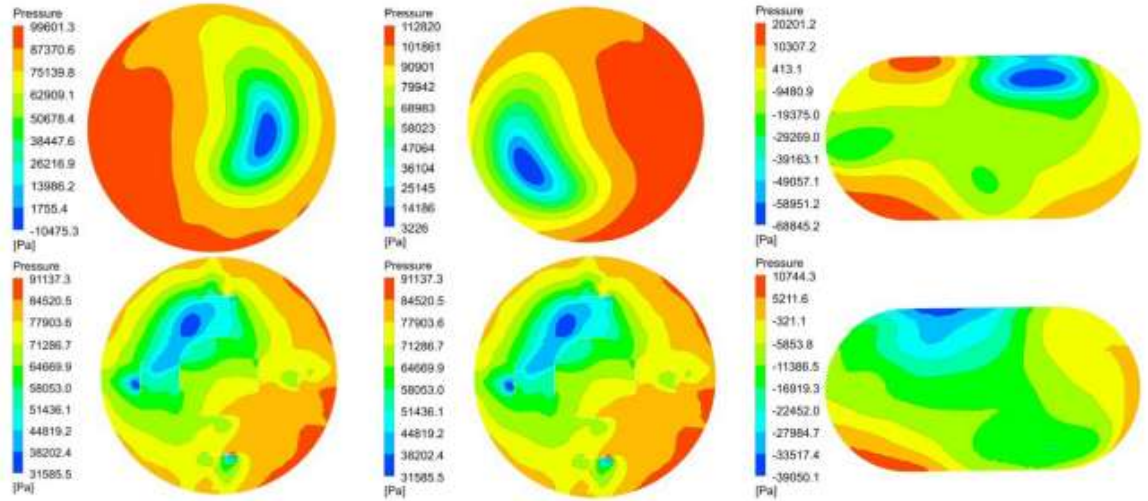


Fig.2.15 Comparison of pressure contours between prototype (upper) and adding flow (lower)(W F Li, 2015).

2.8.2 Water Jet Injection

Group of researchers are now being carried out to investigate the effect of injected water. A novel method injecting an axial water jet from the runner crown downstream into the draft tube cone by (Resiga, 2017.)and the draft tube wall the flow-feedback control technique to supply the jet, using a fraction of the discharge taken from the discharge cone outlet to Mitigation of pressure pulsations in the discharge cone of hydraulic turbines using Flow-Feedback (Constantin TĂNASĂ,2011)

The expected results from the water injection system are presented below by Sebastian Adolfssonwhe study pressure pulsation at draft tube cone (Adolfsson, 2014):

- Reduction in swirl strength
- Reduction in vibrations and pressure pulsations
- Help filling the center of the draft tube and smoothen the velocity profile (boundary layer)
- Better utilization of the draft tube, thus better draft tube efficiency
- Increase in the Francis turbine operating range

- show that this flow control approach successfully removes the vortex breakdown and significantly decreases the overall hydraulic losses in the conical diffuser with swirl(Alin I. BOSIOC1, /2010,)

- The jet increases the axial momentum of flow at the center of the draft tube and decreases the wake of the crown cone and thereby decreases the shear at the interface of the stagnant region and high velocity outer flow, which ultimately results in elimination of the vortex rope by (Foroutan, 2015).

-The method to study the vortex rope by using a water jet issued from the crown tip. The jet is supplied with high-pressure water from spiral case inlet, through the tubular shaft. Romeo SUSAN-RESIGA and Feng Jianjun are being tested at different research environments to mitigate the vortex rope(Susan-Resiga et al., 2011).

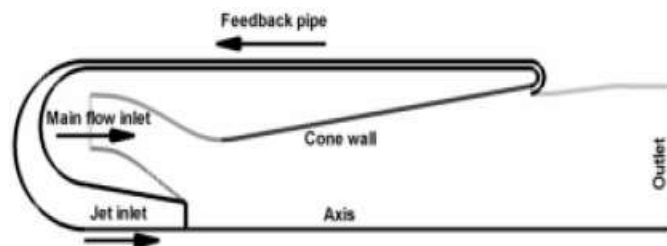


Figure 2.16 Computational domain in a meridian half-plane for the test section with flow-feedback control system(Susan-Resiga et al., 2011).

The jet is supplied with high-pressure water from spiral case inlet, through the tubular shaft see the Figure 2.16. The elimination of severe pressure fluctuations at partial discharge, combined with a significant increase in the draft tube efficiency, compensates the several percent's of the overall turbine discharge that bypass the runner. The vortex rope jet control method is investigated using full 3D unsteady numerical simulation, and the benefits of this novel technique are quantified(C TANASA1, 2016).

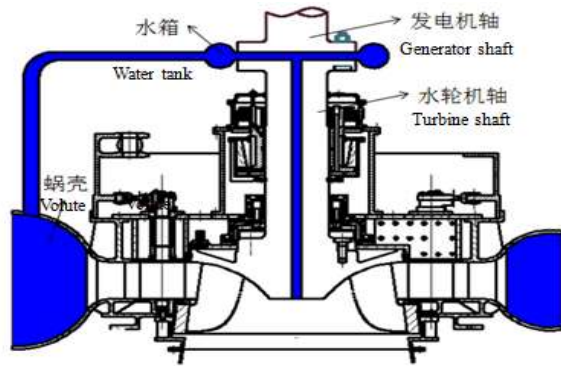


Figure 2.17 Schematic diagram of water replenishment(C TANASA1, 2016).

Chapter III

Research Methodology & experimental

Chapter III

Research Methodology & experimental

3.1 Introduction

This chapter involves physical geometry, prototype domains and meshing domains of draft tube, modeling of fluid turbulence, selection of appropriate boundary conditions, and modeling of transient flow are discussed in detail. Grid resolution and turbulence models chosen from the best unsteady-flow predictions of pressure pulsation and vortex rope will also be applied in the transient-flow simulations then admitted air.

3.1.1 Assumptions

The following assumptions were made for numerical solution:

- Turbulent flow
- Incompressible flow
- Newtonian fluid
- Fully developed flow at the inlet of draft tube at Constant fluid properties
- Smooth walls
- Negligible body forces
- Transient
- Water temperature is at 15°C
- Using ANSYS FLUENT's large-eddy simulation (LES) transient turbulence models in separate simulations.

3.2 Working of CFD Code

In order to provide easy access to their solving power all commercial CFD packages include sophisticated user interfaces input problem parameters and to examine the results of draft tube flow. Hence all codes contain three main elements

1. Pre-processing
2. Solver
3. Post –processing.

3.2.1 Pre-Processing

In pre-processing it consists of input of a flow problem by means of an operator friendly Interface and subsequent transformation of this input into a suitable form which can be used by the solver ANSYS fluent for pre-processing in which domain, materials and boundary conditions were defined. First simulation water was selected as working fluid and reference was taken as 1 atmospheric pressure. Second simulation mixture of water and air and Turbulence plays an important role inside the draft tube. Hence, large-eddy simulation (LES) model was defined to analyze the flow inside the draft tube and kinetic energy transport at sub grid.

- Defining the geometry of the region for computational domain.
- Generating the Grids for subdivision of the domain into a number of smaller, non-overlapping sub domains.
- Specifying the appropriate boundary and continuum conditions at cells, which coincide with or touch the boundary?

3.2.2 Solver

High resolution advection scheme with second order turbulence numeric was used. Auto timescale control and RMS (Root Mean Square) criteria was specified. Maximum iterations were increased accordingly. The majority of post-processing jobs were carried out using the built-in post-processing tool ANSYS fluent.

3.2.3 ANSYS-FLUENT CFD Code

ANSYS-FLUENT, a commercial CFD solver, provides comprehensive modeling capabilities for a wide range of incompressible and turbulent fluid flow problems in draft tube. Transient analyses can be performed with this code. ANSYSFLUENT contains the broad physical modeling capabilities needed to model flow, turbulence for draft tube cone application. Several turbulence models are implemented in ANSYS-FLUENT making it a proper choice for the present simulations of draft tube(Guide, 2013).

Two numerical approaches are available in ANSYS-FLUENT: density-based solver and pressure-based solver. In the method of the pressure field is obtained from the

momentum transport equation. On the other hand, in the pressure-based approach, the pressure field is extracted by solving a pressure or pressure correction equation which is obtained by manipulating the continuity and momentum equations. Based on the physics of the current problem the pressure-based solver is used. Since the governing equations are nonlinear and coupled, the solution process involves iterations where in the entire set of governing equations is solved repeatedly until the solution converges, i.e., the solution residuals become smaller than a predefined threshold(Guide, 2006).

3.3 Draft Tube Geometry and Domain

3.3.1 Geometry

The draft tube geometry includes spiral case and the draft tube cone, the 90 ° elbow, the diffuser with one pier and spiral case as shown in figure (3.1) and draft tube dimensions shown in figure (3.2), then draft tube specification dimensions in table (3.1)

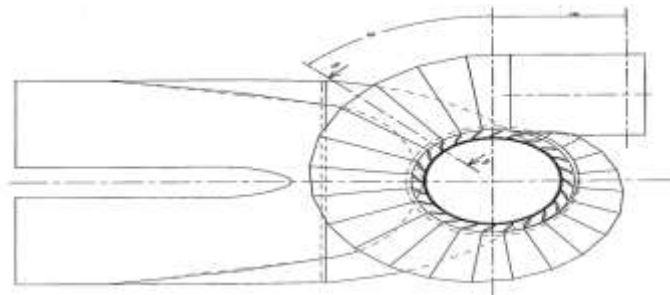


Figure 3.1: spiral case and draft tube

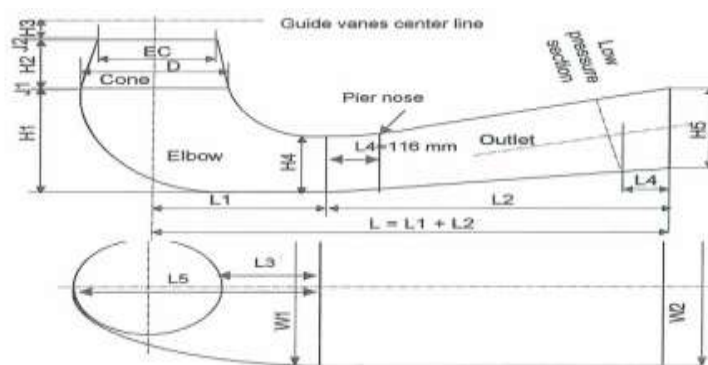


Figure 3.2: M.D.draft tube geometry

Table 3.1: drafts tube dimensions

	Name	Value(m)
Cone	EC	6
	D	7.54
	H2	3.6
Elbow	D	7.54
	L3	5.66
	L5	13.2
	L1	9.4
	H1	10.5
	H4	4.3
	W1	18
Outlet	L2	17.7
	H4	4.3
	H5	6.9
	W1	18
	W2	18.3

The domain used in the simulations is in the same real scale as the prototype turbine and draft tube in the field (M.D. Hydro power unit two), which can be seen in figure 3.3

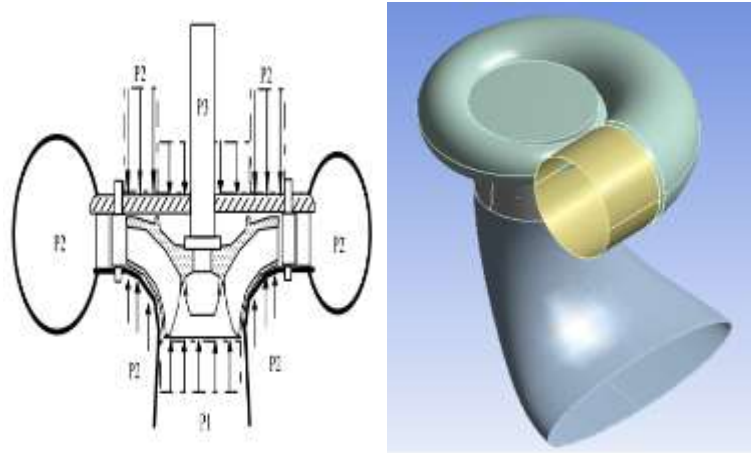


Figure 3.3: The draft tube and spiral case domain.

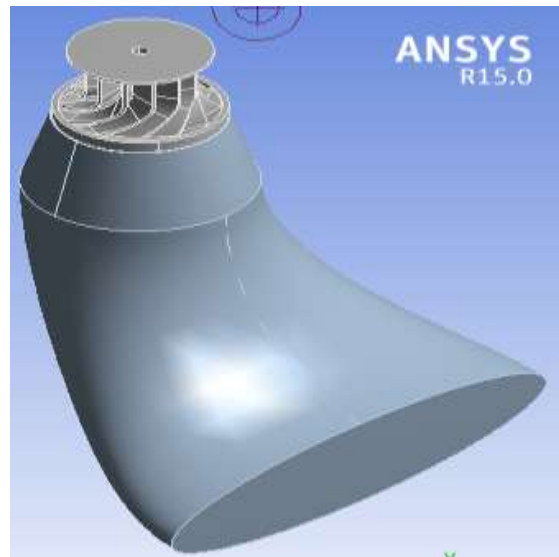


Figure 3.4: The draft tube and runner domains

According to standard, the model must maintain the geometric and hydraulic similarity with the prototype. The hydraulic similarity of a geometrically similar model and prototype can be determined using Equations (3.1), (3.2) and. Hydraulic performance of model turbine is directly transposable to the prototype with scale formula which covers the guaranty given by the supplier of the turbine.

$$(Q_{ED})_p = (Q_{ED})_M \quad 3.1$$

$$N_{ED} = n_{ED} \quad 3.2$$

The discharge factor Q_{ED} and speed factor n_{ED} , can be computed as,

$$Q_{ED} = \frac{Q}{D^2\sqrt{E}} \quad 3.3$$

$$n_{ED} = \frac{nD}{\sqrt{E}} \quad 3.4$$

Where, Q is the discharge in $\text{m}^3 \text{s}^{-1}$, D is the reference diameter of runner in m, E is the specific hydraulic energy in Jkg^{-1} , n is the rotational speed of the runner in s^{-1} .

3.3.2 Draft Tube Domain

By using technical drawings of the draft tube, it is regenerated in ANSYS, and adapted for optimal meshing. The geometry created in Solid work contains only the cone and elbow surface of the draft tube. The 3D ICEM of the draft tube evolution and cross-section area of the draft tube from inlet to outlet Figure 3.4. The draft tube was equipped with a transparent cone (see Fig. 3.5).

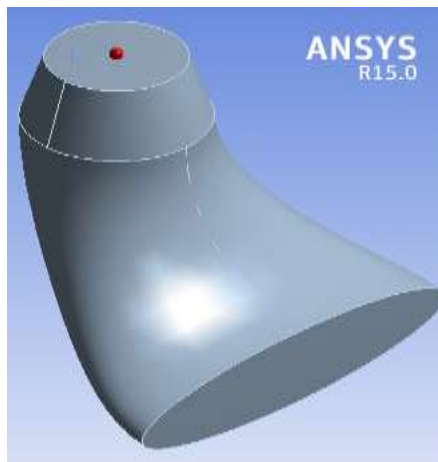


Figure 3.5: The 3D draft tube geometry from the M.D. Hydro power plant

The inlet of the draft tube, shown in figure 3.5 is not a plane surface. This is done to improve the computation conditions for the model assembly. The center of the inlet is covered with a circular surface, which will be used as the rotating tip of the runner hub. The runner is a rotating domain in the computations, while the draft tube is stationary. By connecting the runner outlet and draft tube inlet close to the runner blades, the effects of the

rotating runner domain on the stationary area below the blades is reduced. Draft tube cone accessory door is eliminated but the elbow is added in CFD for simulation Figure 3.6. Figure 3.7 the draft tube Top view and Side view

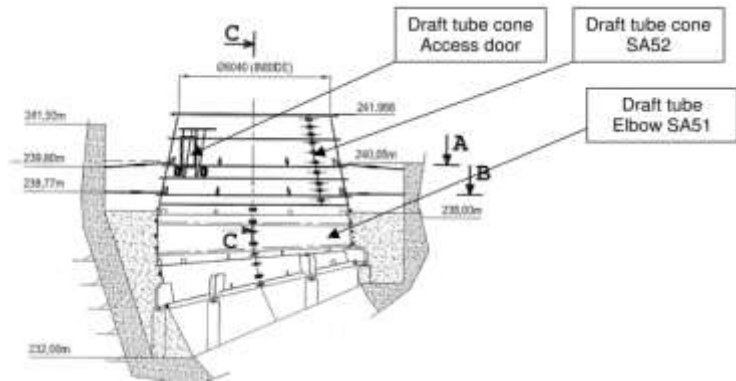
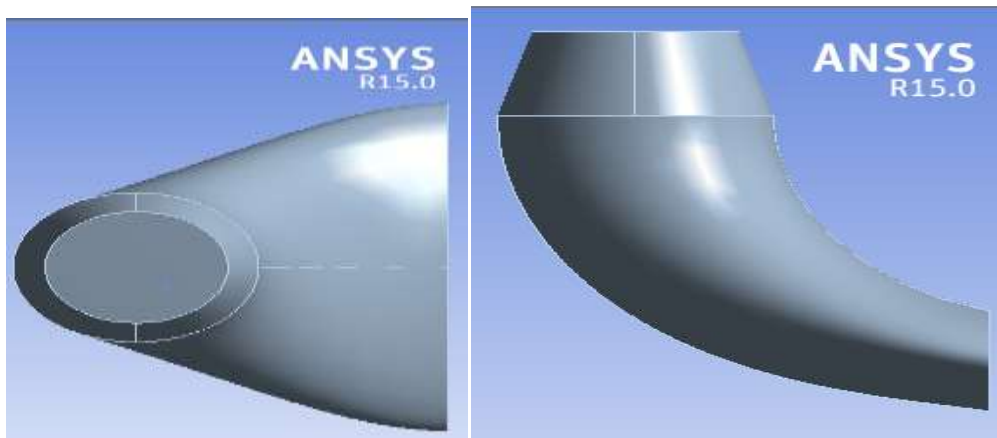


Figure 3.6: Draft tube cone accessory door



(a) (b)

Figure 3.7: The draft tube (a) Top view (b) Side view

3.4 Runner

The runner is the essential part from the hydraulic standpoint since its layout conditions the unit performances. The runner is consisting of a welded construction technology with cast parts (runner crown, band and blades), for General runner characteristics show table (3.2) below.

The runner is designed and fabricated at the ALSTOM Waterpower Laboratory at France. As the geometry files are not compatible with ANSYS fluent, the geometry is exported from solid work and regenerated for optimal meshing. Figure 3.8 shows the runner geometry from solid work, and the new geometry created in ICEM. The original geometry contains a detailed geometry of the solid part of the runner, while the new geometry is a detailed geometry of the waterways of the runner.

Table 3.2 Runner dimensions Characteristics

Mechanical part	Characteristics
Runner outlet diameter	6020 mm
Direction of rotation	Clockwise rotation
Runner height	3669 mm
Maximum diameter	6100 mm
Number of blades	13
Weight	98900 Kg
Upper and lower wearing rings	Upper :Shrunked and bolted to the runner Lower

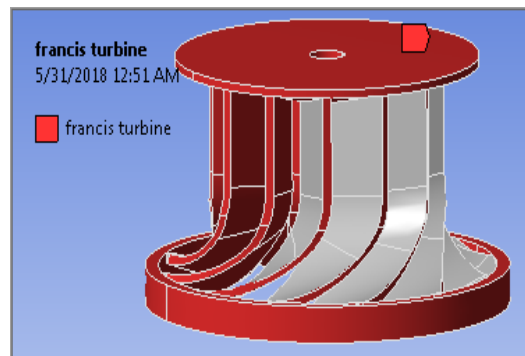


Figure 3.8: The M.D. hydro power model runner geometry in ANSYS

3.5 Flow Domain

The flow domain for the current CFD study is based on the 1:10 scale prototype, and the geometric shape of which is closely similar to the existing draft tube used in the Merowe hydro power plant. Modeling of the turbine draft tube at full- scale Reynolds numbers was not practical for this analysis due to large amounts of computational time and resources required to get reliable and consistent results. The difficulty in obtaining detailed measurement data to validate the CFD model in the full scale field tests was another major reason for employing prototype -size model in the CFD simulation. The tiny corner fillet in the rectangular section of the draft tube and the sliver surface below the inlet cone were not modeled due to meshing difficulties. The support pier downstream of the draft tube was also excluded for simplicity. The flow domain has been rotated (0,0,0) about the inlet plane to make it identical to the prototype.

3.5.1 Create Named Selections for the Geometry Boundaries.

In order to simplify the work later on in ANSYS Fluent, should label each boundary in the geometry by creating named selections for the runner and draft tube inlets, the outlet, (the outer wall boundaries are automatically detected by ANSYS Fluent).

- a. Select the runner (runner crown, band and blades) in the geometry that is displayed in the ANSYS Meshing application.
- b. Right-click and select the Create Named Selection option. (rotational runner) Inlet water.
- c. Smooth draft tube.

Outlet pressure

3.6 Mesh Generation

The meshing of the draft tube flow domain is generated in ANSYS ICEM CFD as shown in fig.3.9 The mesh generation is done to convert the large domain into number of small elements. Each element consists of nodes at which flow variables are calculated(Harris, April 2013). The unstructured triangular elements on surfaces and tetrahedral in flow domain are adopted in draft tube meshing. The fine mesh is done near

the surfaces in order to capture the turbulence as compared to interior domain(Kamkar, 2011). This has reduced the number of grids points and hence computational time.

The mesh will be read in and displayed, and the zones will be shown in the TUI window. Mesh generation is an essential first step in numerical flow solutions. A poor quality mesh can adversely affect the stability and accuracy an achieved. Overall, the meshing problems faced in this work are caused by the complex geometry and the limitations of the wall distance imposed by ANSYS FLUENT as part of its turbulence modeling and near-wall treatment.

The use of proper wall element size is vitally important for the turbulent flow studied here. The wall elements may fail to work correctly if their sizes are either too large or too small. Element type and mesh topology can have a considerable impact on course grid solutions, and may affect the mesh resolution required to achieve a grid-independent solution.

To improve computational efficiency, the number of extension nodes was reduced by gradually increasing the mesh sizes through an exponential growth.

3.6.1 Mesh Type and Topology

Unlike some simple linear geometry, the strong curvature of the draft tube can incur more adverse pressure gradients in which flow separations may occur. Accurate simulation of the flow phenomena in the draft tube requires computational grids that simultaneously capture the geometric curvature and discontinuities in the solution.

A non-uniform tetrahedral mesh generated by ICEM CFD was used for the current simulations because it is best suited for adequately resolving the near-wall region of the flow field. In fact, no meshing algorithm up to date can guarantee a triangulation of a domain without creating any small angles that are not already present in the input domain.

3.6.2 Mesh Quality

Set basic meshing parameters for the ANSYS Meshing application. For this analysis, you will adjust several meshing parameters to obtain a finer mesh.

- a. In the Outline view, select Mesh under Project/Model to display the Details of “Mesh” view below the Outline view.
- b. Expand the Sizing node by clicking the “+” sign to the left of the word Sizing to reveal additional sizing parameters.
 - i. Change Relevance Center to Fine by clicking on the default value, Coarse, and selecting Fine from the drop-down list.
 - ii. Change Smoothing to High figure (9)

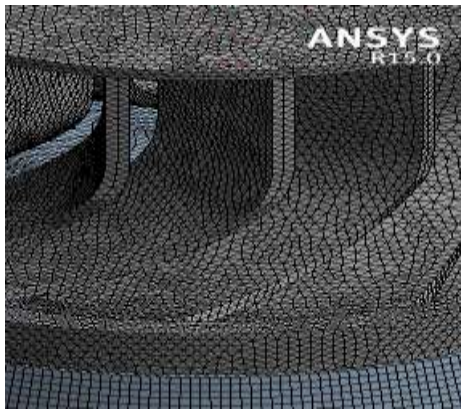


Figure 9: Mesh Quality

- c. Add a Body Sizing control.
 - i. With Mesh still selected in the Outline tree, click the draft tube in the graphics display to select it.
 - ii. Right click in the graphics area and select Insert → Sizing from the context menu. A new Body Sizing entry appears under Mesh in the project Outline tree
 - iii. Click the new Body Sizing control in the Outline tree.
 - iv. Enter $8e-2$ for Element Size and press Enter. Figure (10)



Named selection

Body Sizing

Figure 10

Right-click Mesh in the project Outline tree, and select Update in the context menu.

3.7 Grid sensitivity analysis

To evaluate the grid sensitivity, several meshes are created with an increasing number of nodes for both the runner and the draft tube. Due to limitations in computer memory, a limit of combined nodes is set at 1,500,000 nodes. 3D computational domain consists of 2,028,000 structured cells. In both cases the grids are refined near the wall as well as near the center of the draft tube as shown in Fig. 10. Grid sensitivity analysis in this study shows that non refined grids result in convergence problems and as high as 10% error in predictions.

3.8 Boundary Condition of Modeling

Transient flow calculations for the elbow draft tube rely heavily on the precision of the appropriate boundary conditions. Information on the dependent flow variables at the domain boundaries must be properly specified in order to obtain a unique solution for the problem. Poorly defined boundary conditions can have a significant impact on the accuracy of the CFD solution, no matter how fine the discretization or how sensible a turbulence model. This is particularly true for the present study since only the draft tube component of the Francis turbine is examined here.

The approach essentially ignores all variability outside the truncated integration flow domain. To get a realistic solution, experimental data is still needed to determine the

inlet and outlet boundary conditions for the draft tube flow. The boundary conditions have been carefully determined here to prevent the over-specifying or under specifying

$$\dot{m} = Q\rho \text{ kg/s}$$

3.5

Table 3.3: Mass flow values for the operating points in fluent

Part load	Case A 45 (m)		Case B 35 (m)		Case C 33 (m)	
	Ga.(deg)	\dot{m} (kg/s)	Ga.(deg)	\dot{m} (kg/s)	Ga.(deg)	\dot{m} (kg/s)
0.5Q _{BE} p	15.9	130732.2	17.8	127147.8	18.3	126649.9
0.6Q _{BE} p	18.7	156818.9	21.3	152537.5	22	151940.1
0.7Q _{BE} p	21.7	182955.4	24.0	177927.2	25.1	177329.8
0.8Q _{BE} p	24.5	209091.9	27.8	203416.5	28.4	202620
0.9Q _{BE} p	28.2	235228.4	31.2	228806.3	32.7	228009.7
Q _{min}	29.7	248918.9	35.0	243542.3	35	243442.7
Q _{BEp}	31.3	261364.9	35.8	254295.6	36.6	253299.9
Q _{max.}	33	273810.8	37.4	264949.3	33.2	263157.1

3.9 Inflow Plane

The boundary treatment used for the inflow plane is the so-called "capacitive boundary condition". An experimental profile for the mass flow was specified at the inlet to account for the boundary layer effects. Flow angle normal to the boundary surface is

employed because the inlet swirl is modeled in this project. For transient operations, the same shape of the inlet velocity profile is assumed in order to evaluate the instantaneous total pressure distribution at the inlet. The assumption of isothermal and incompressible flow conditions eliminated the temperature and density gradient effects.

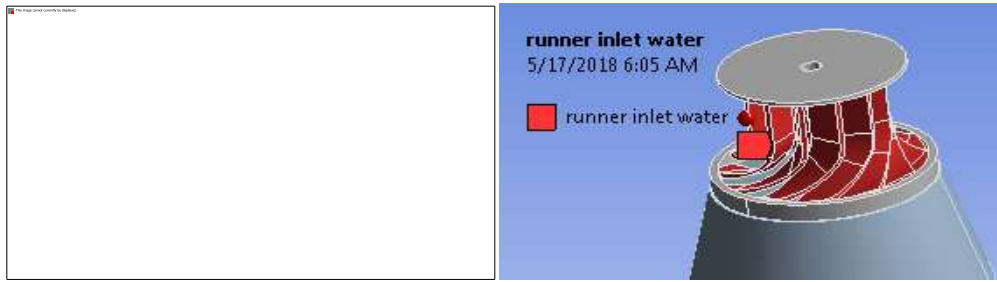
A constant turbulence intensity of $I = 5\%$ was applied at the inlet. The turbulence kinetic energy (k) was calculated from this specified intensity via the relationship $k = 1.5 I^2 U^2$ [m^2/s^2] for isotropic conditions. The turbulence dissipation rate (ϵ) [m^2/s^3] was approximated via the relationship $\epsilon = K^{3/2}/I \cdot 0.3 D_h$ where D_h is the hydraulic diameter of the inlet. The turbulent length scale is determined automatically by the code. The approach of determining the dissipation rate based on experimental results was not used here because of the large variation and limited published data available for draft tube analysis.

At the inlet section, the radial profiles of axial and circumferential velocity components as well as turbulent kinetic energy are obtainable from the mean circumferentially averaged experimental data by interpolation. Turbulence dissipation rate is usually difficult to measure and thus is not available from experiments. Here, the inlet profiles for the dissipation rate are computed from the turbulent kinetic energy profiles as $\epsilon = k^{3/2}/l$. The turbulence length scale $l = 0.01R$ (R is the runner radius). Profiles of the specific dissipation rate at the inlet are obtained from $\omega = k^{1/2}/(C_\mu l)$ with $C_\mu = 0.09$.

3.9.1 Runner Boundary Conditions

The runner domain, shown in figure (3.7) is to rotate about the z-axis. The speed of rotation is defined by the operating point being simulated.

The hub, shroud, and blades of the runner are set as smooth walls. Because they are part of the rotating domain, they will automatically rotate at the same rpm as the domain. Figure 3.11(a) shows the walls of the runner. Figure 3.11(b) shows the runner inlet. The inlet boundary conditions depend on the operating point. Table 3.3 shows the mass flows for the three operating points.



(a)

(b)

Figure 3.11 (a) smooth wall runner (b) inlet water boundary condition

3.9.2 Outflow Plane

The boundary treatment used at the outlet is closely related to the boundary conditions specified at the inflow plane. The outlet condition must be carefully defined, as the disturbances introduced at an outflow boundary can propagate upstream and have an effect on the entire computational region. Total pressure cannot be used to specify the outflow condition, as it is unconditionally unstable when the water flows out of the domain.

For unsteady-flow operation, a constant static pressure boundary condition was established. The buoyancy effects were neglected as they played no significant role in the current problem. The outlet flow direction was left unspecified, and to be determined by the local pressure field computation. The other flow variables on the outlet boundary surface were extrapolated from the interior by the computation. For unsteady-flow simulations, the outlet total pressure was imposed as a function of time.

Neumann boundary conditions are imposed such that the turbulence quantities are assumed to have a zero normal gradient at the outlet. At the outlet section the radial pressure equilibrium ($\partial p / \partial r = \rho V_{2\theta} / r$) is applied, which is the reduced form of the radial momentum conservation equation.

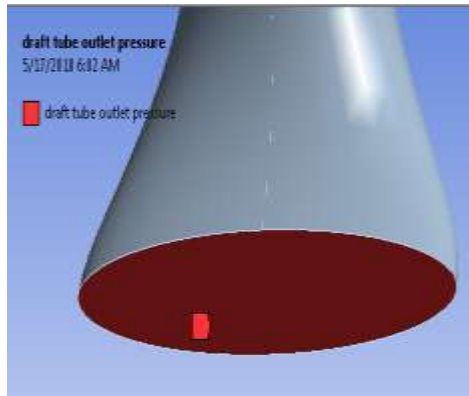


figure 3:12 outlet boundary condition

3.9.3 Wall Boundary

A smooth wall boundary condition was applied at the surfaces of the inlet extension draft tube. A non-slip adiabatic heat transfer flow condition was imposed at the wall. The flow immediately next to the wall assumes the zero wall velocity. The effect of surface roughness was not studied here, even though it may have some influence on the loss mechanism and the efficiency of the full-scale draft tube. The automatic near-wall treatment in ANSYS FLUENT was used when an ω -based turbulence model was applied. No-slip conditions are applied at wall boundaries figure 3.13

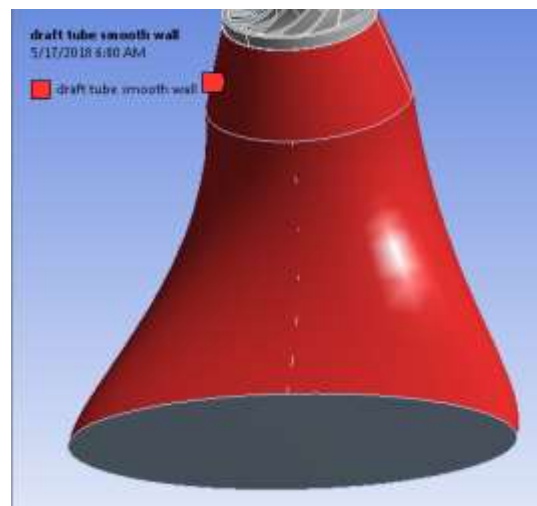


figure 3:13 smooth wall boundary condition

3.9.4 Runner-Draft tube Interface

interface between the runner and the draft tube, shown in figure 3.14, is a critical part of the simulation. The interface consists of the runner outlet on one side, and the draft tube inlet on the other side. The connection is a general connection with a frozen rotor. In order to get the effects of the runner rotation in the draft tube flow, the pitch change is set to none.



Figure 3.14: Domain interface between runner and draft tube

3.10 Turbulence Model and Transient Simulations

3.10.1 Large Eddy Simulations (LES)

Turbulent pulsations in the draft tube are always three-dimensional and unsteady, and consist of eddying motion with a wide range of length scales. The following subsections briefly highlight some important features of the details on the structure of turbulent flows, such as pressure pulsations, can be obtained by LES. LES is an approach which solves for large-scale pulsations motions and uses »sub-grid« scale turbulence models for the small-scale motion. In ANSYS three LES models are available: the Smagorinsky model, the wall-adapted local eddy-viscosity model (LES WALE) and the Dynamic model. The first two models are algebraic. The Smagorinsky model is available together with two different formulations of the wall damping function. The LES WALE model needs no wall damping, while the Dynamic Smagorinsky-Lilly model uses the information contained in the resolved turbulent velocity field to evaluate the model coefficient. The method needs explicit (secondary) filtering and it is therefore more time consuming than the algebraic models. LES requires fine grids and small time steps,

particularly for wall bounded flows, as well as a large number of time steps to generate statistically meaningful correlations for the pulsations velocity components.

3.10.2 Advection Scheme

The steady state simulations use a high resolution advection scheme, while the transient simulations use the upwind advection scheme.

3.10.3 Convergence Criteria

The convergence criteria for the unsteady the MAX residuals, while the transient simulations are set at 10^{-5} for the RMS residuals. In case there are convergence problems due to the unstable nature of the draft tube flow, the pressure difference from inlet to outlet is monitored. If the residuals do not converge, but the pressure difference stabilizes, the general behavior of the draft

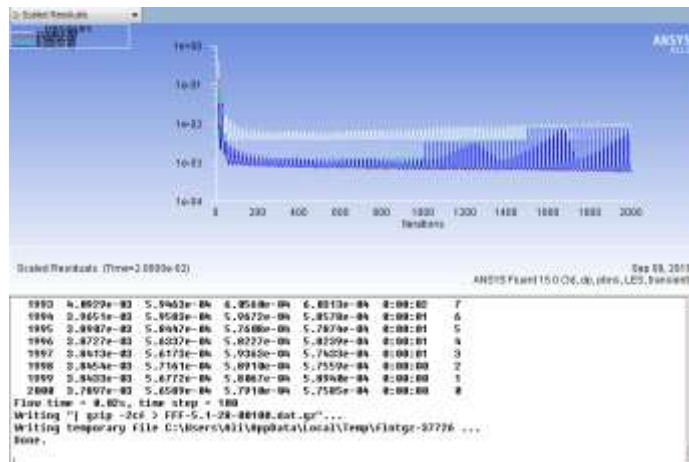


Figure 3.15: data solution

3.11 Air Supply Simulations

One of the most widely used methods to reduce the pressure pulsations and the vortex rope is the injection of air into the runner or draft tube. Air can be admitted in several locations including the spiral case, the annular chamber between the wicket gates and the runner, the draft tube wall, the runner band, the runner crown cone, or a snorkel attached to the runner cone both the location and the quantity of air have significant effects

on the efficiency of the unit. For high tail water units, where the most severe pulsations occur, compressed air must be injected into the draft tube since the pressure below the runner is more than the atmospheric pressure.

The main requirements and guidelines for a successful location to control pulsations and the vortex rope are:

- The location should address the cause of the vortex rope formation, rather than just its effects such as pressure pulsations.
- The pulsations and the vortex rope should be controlled at the inlet of the draft tube.
- The method should focus on the stagnant region near the axis of the draft tube rather than the swirl near the wall.
- The method should not affect the efficiency of the machine when operating at or near the best efficiency point.
- Position of air intake to minimize pressure location through air pipes, necessary to know the amount of air flow needed to decrease pulsations and the vortex rope.

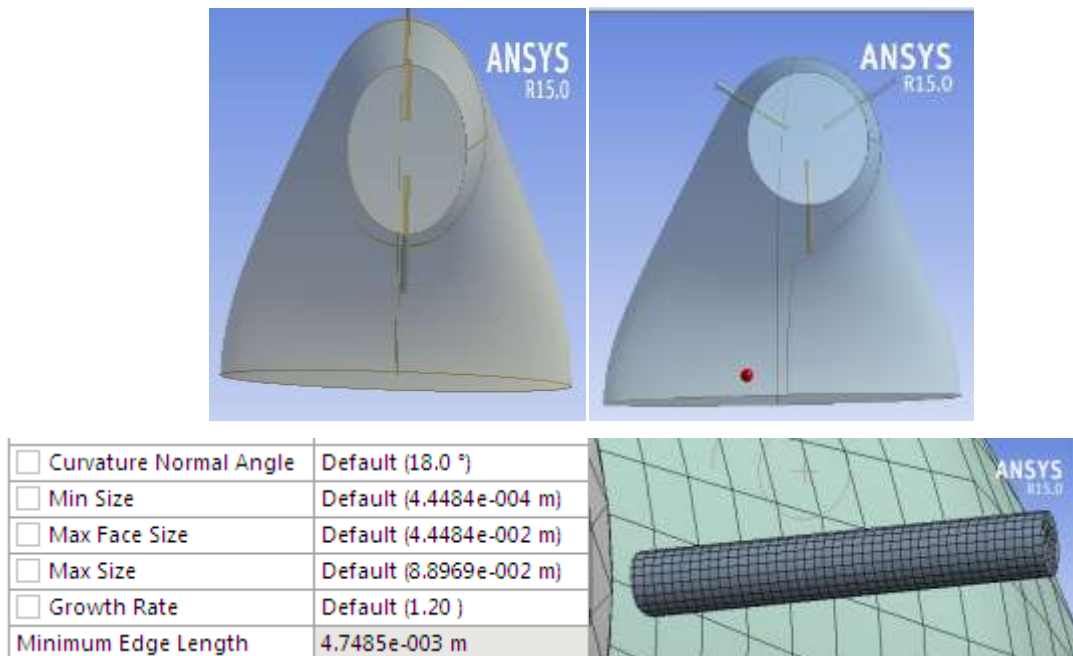


Figure 3.16: Air injection path

In this study, the mixture model is used for the simulations of the internal flow with air admission in the draft tube, which assumes the two phase flow is a homogeneous mixture whose density can be described as

$$\rho_m = \alpha_a \rho_a + (1 - \alpha_a)\rho_L \quad 3.6$$

Where α is the volume fraction. The subscripts of m, a, and L indicate the mixture, air, and liquid components, respectively.

3.12 Summary

The Francis turbine and draft tube models of M.D. hydro power project were investigated numerically. The main reason for choosing this test case was the availability of accurate and detailed measured data for several operating conditions. The primary challenge, however, was that the geometry of the draft tube is not available in open literature. Therefore, combining data from several documents, the geometry of the M. D. hydro power draft tube is obtained. Within the present research study, the simplified M. D. hydro power draft tube is investigated first with results being presented in. Then, the complete cone and elbow draft tube is numerically investigated. The meshing of the draft tube and input boundary conditions requirements in this chapter.

Air admission can also be made through pipes mounted at the draft tube cone, this admission technique mainly concerns problems with pressure pulsations and vortex rope but may due to its simple installation procedure provide with an easy solution in some special flow problems.

Chapter IV

Results and Discussion

Chapter IV

Results and Discussion

4.1 Introduction

These undesirable phenomena may occur individually or in combination in hydroelectric plants. Therefore, control or elimination of the vortex rope is necessary for improving hydropower plant efficiency and preventing structural vibrations.

Air injection uses two mechanisms (180° and 120°) have been used to control the draft tube pressure pulsations vortex rope. Furthermore, since there is not yet a general agreement on the main causes that lead to self-induced instabilities in a swirling flow, the practical solutions sometimes have different results.

According to the objectives of this study, three operating conditions are selected covering a wide range (70%, 60% and 50% of the BEP flow rate) of operating conditions. Table 4.1 summarizes the characteristics of these three operating points. The points of interest are selected for the same head (energy) coefficient of $\psi = 0.65$. The energy coefficient increase with head increase table (4.2). And different flow rate coefficients of $\phi = 0.41, 0.368, 0.34, \text{ and } 0.26$ corresponding to about 70%, 60% and 50% of the flow rate at the BEP. The discharge coefficient at part load decrease when part load flow increase and decrease when head decrease show table (4.3)

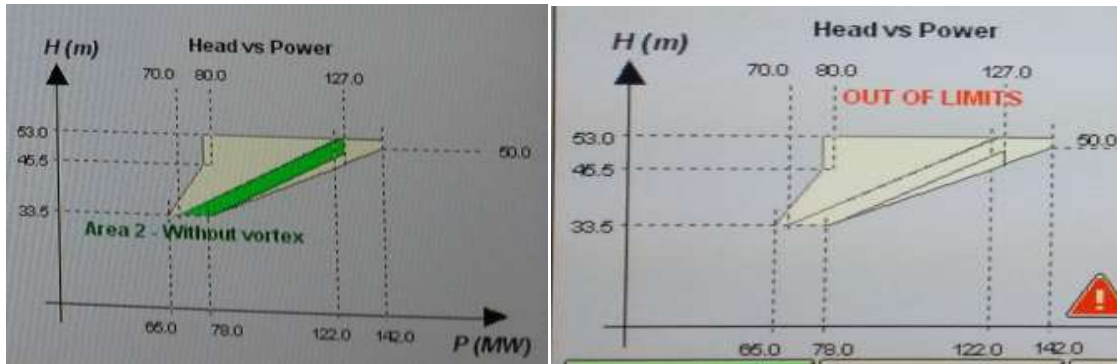
Table (4.1) discharge description

Case	H(m)	Q_{\max} (m ³ /s)	Q_{BEP} (m ³ /s)	Q_{\min} (m ³ /s)	N (rpm)	D (m)
A	45	275	262.5	250	100	6
B	35	266.07	255.355	244.64	100	6
C	33	264.2827	254.3914	244.5	100	6

4.2 Description of the M.D.Hydro Power Part Load Operation Zone

The simulation in partial operation condition in M.D hydro power plant unit two in critical head 33 m and a range part load from $0.7 Q_{\text{BEP}}$ to $0.5 Q_{\text{BEP}}$. In figure (4.1) showed the M. D hydro plant operation zone figure (4.1) (a) which characteristics by green (operation without vortex) and figure (4.1) (b) operation out of limit zone (operation with vortex). At full load operation flow rate is greater than Q_{\max} , at and partial load flow rate is less than Q_{\min} . Q_{BEP} the operation in limit (designed operation) see table (4.1) is discharge

description. There are three operations constant rotational speed (N) rpm, runner diameter (D) m and runner blade angle



(a) operation without vortex zone

(b) operation out of limit zone

Figure (4.1) M.D hydro plant operation zone

4.3 Reynolds Numbers, Discharge Coefficient (ϕ), Swirl Number (S)

Operations were performed with one runners for all cases, and data were collected at 33 m operating head at 6 different wicket gate settings. All of the collected data are included in tables above. Quantitative analysis was restricted to the dominant swirl. The corresponding Reynolds numbers based on the runner's diameter (6 m) and angular velocity is 8.4×10^6 at 100 rpm. Therefore, it is only relevant parameter for the operating points considered in this study are the turbine's discharge coefficient. The swirl number is the ratio between the circumferential and the axial momentums, and is defined in this case at the inlet as with R being the runner's radius, $R = D/2$, and V and U denoting the mean circumferential and axial velocities respectively. The inlet swirl number at the BEP is found to be about 0.17 while it increases dramatically as wicket gates are further closed (part-load operating conditions), namely to the value of 0.91 and 1.03 and 1.05 for cases A, B and C respectively table (4.3). The head 33 has low energy coefficient see table (4.4).

Table (4.2) discharge coefficient

Part load	Case A			Case B			Case C		
	Ga.(deg)	Q(m ³ /s)	Φ	Ga.(deg)	Q(m ³ /s)	ϕ	Ga.(deg)	Q(m ³ /s)	ϕ
0.5Q _{BEP}	15.9	131.3	0.148	17.8	127.7	0.144	18.3	127.2	0.143
0.6Q _{BEP}	18.7	157.5	0.177	21.3	153.2	0.172	22	152.6	0.172
0.7Q _{BEP}	21.7	183.75	0.207	24.0	178.7	0.201	25.1	178.1	0.200
0.8Q _{BEP}	24.5	210	0.236	27.8	204.3	0.230	28.4	203.5	0.229
0.9Q _{BEP}	28.2	236.25	0.266	31.2	229.8	0.259	32.7	229	0.258
Q _{min}	29.7	250	0.281	35.0	244.6	0.275	35	244.5	0.275
Q _{BEP}	31.3	262.5	0.296	35.8	255.4	0.287	36.6	254.4	0.286
Q _{max.}	33.2	275	0.310	37.4	266.1	0.300	33.2	264.3	0.298

Table (4.3) Swirl number (S)

	Case (A)	Case (B)	Case (C)
0.5Q _{BEP}	0.91	1.03	1.05
0.6Q _{BEP}	0.58	0.66	0.68
0.7Q _{BEP}	0.39	0.48	0.49
0.8Q _{BEP}	0.27	0.34	0.36
0.9Q _{BEP}	0.18	0.23	0.25
Q _{min}	0.14	0.11	0.20
Q _{BEP}	0.11	0.14	0.17
Q _{max.}	0.08	0.13	0.15

Table (4.4) The energy coefficient.

	H _m	2gH	$(\omega D/2)^2$	Ψ
C	33	647.13	986.95	0.65
B	35	686.35	986.95	0.69
A	45	882.45	986.95	0.89

4.4 Draft Tube Flow Post-Processing

This is the final step in CFD analysis, and it involves the results and interpretation of the predicted flow data. FLUENT software includes full post processing capabilities and exports CFD data to third-party post-processors and visualization tools the main outcomes of post processing is LES.

4.5 Numerical Prediction of Part Load Operation

Prediction of Pressure Pulsation Amplitudes and vortex rope for Different Operating Regimes Shape of the vortex rope at BEP, 70%, 60% and 50% is presented as

contours and flow streamline can be displayed of constant pressure figures below a pressure pulsations and vortex ropes were observed at 50% of BEP. The whole range of variable values will be divided into a number of contours, each covering a range of values. The main settings required are locations and variable.

4.5.1 Draft tube cross section contours

A contour plot is a series of lines linking points with equal values of a given variable, or points within a narrow range of values. The whole range of variable values will be divided into a number of contours, each covering a range of values. The main settings required are Locations and Variable. Figure 4.2 (a) the vertical section at center of draft and (b) shows the pressure contour on the cross section of the draft tube. The BEP pressure contour shows a variables pressure zones at the tip of the draft tube section.

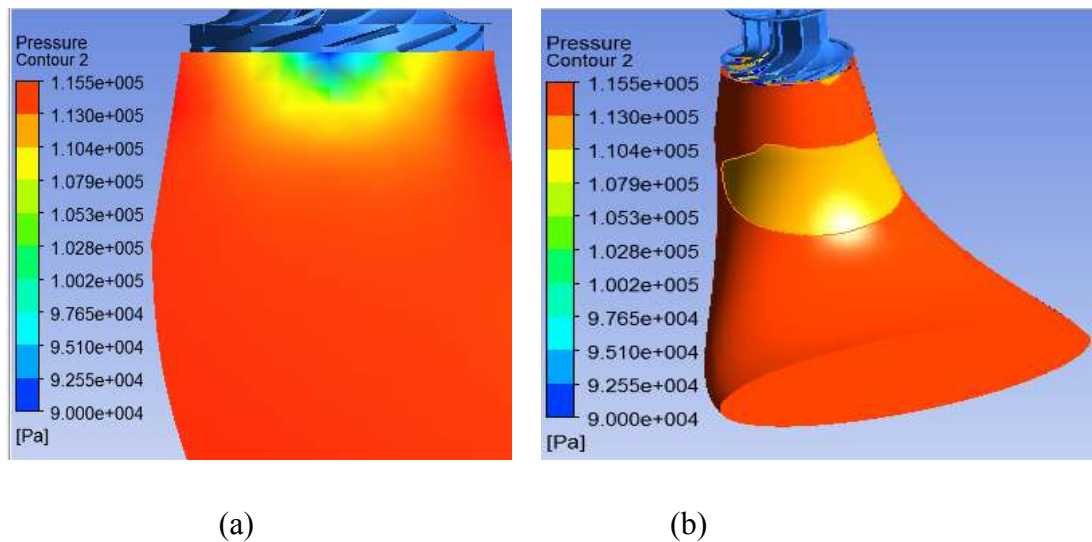


Figure 4.2: Pressure contour at the cross section of the draft tube at BEP

The range of the color map has been set and reduced so that only the dissipation inside of the volume is visible, because the highest value of dissipation occurs in boundary layer regions.

4.5.2 Draft tube Section at Operations at Part Load 70%, 60% and 50% Q_{BEP}

We see in Figure 4.3 that the instability flow in the draft tube forms a pressure pulsation that attaches to the runner crown. As shown the variation of pressure region in the core of the draft tube cone inlet suction. As the discharge is decrease near the band, the pressure value in the core is decrease also.

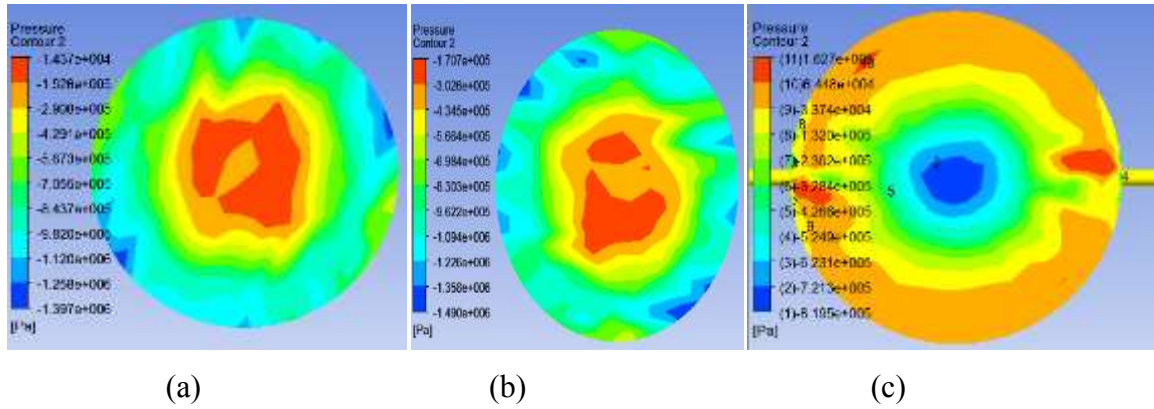


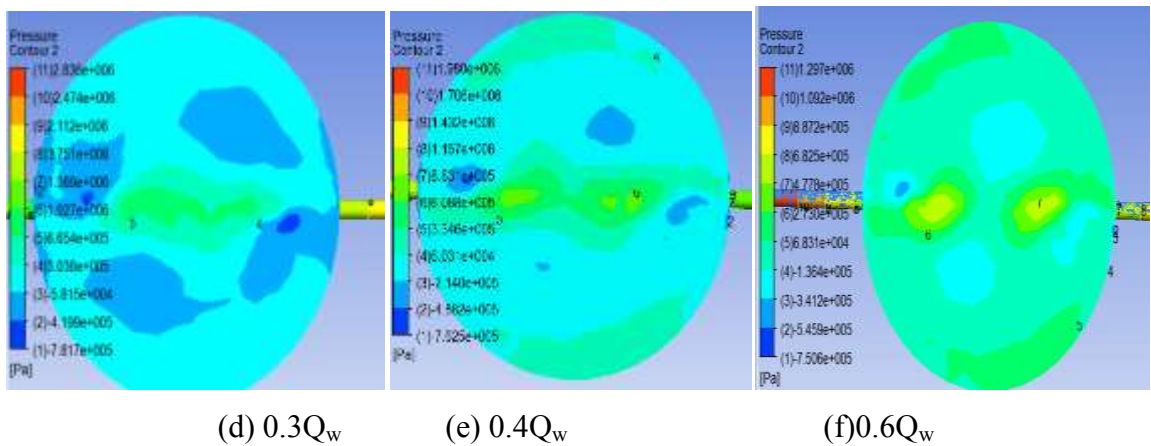
Figure 4.3 Operations at part load (a) 70% Q_{BEP} (b) 60% Q_{BEP} (c) and 50% Q_{BEP} s in the draft tube

4.6 Air injection System 180°

4.6.1 Pressure Distribution at Draft Tube Inlet Horizontal Section

Air will mitigate to the low pressure zones in the flow, drastically changing the pressure dynamics in the flow along its path. The air path is mainly determined by the flow pressure and the location of injection points. At $0.6Q_w$ the pressure pulsations are reduced after admitted high air pressure Figure 4.4.

It can be seen that the low-pressure zone becomes smaller when air admission is conducted, and air admission changes the location of the low pressure zone at a draft tube horizontal section. For the case of air admission from the draft tube cone wall holes, the pressure levels at both sections arise for larger air ventilation, i.e.

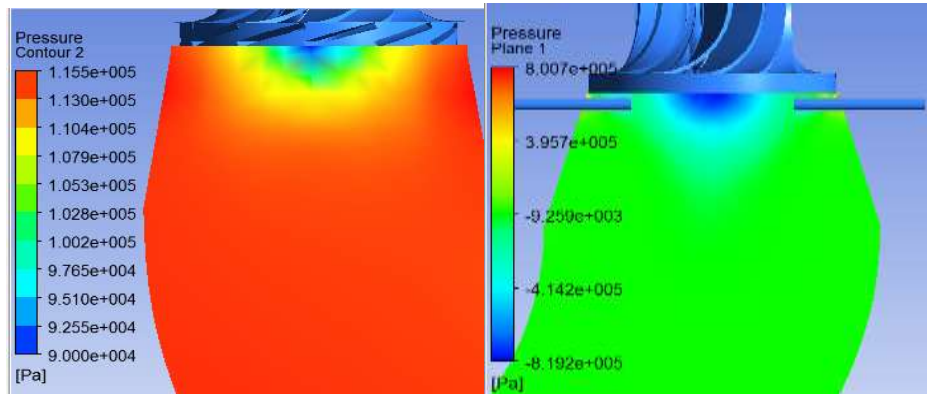


With air admission 50% Q_{BEP}

Figure 4.4: pressure distribution in draft tube inlet horizontal section

4.6.2 Pressure Distribution at Draft Tube Inlet Vertical Section

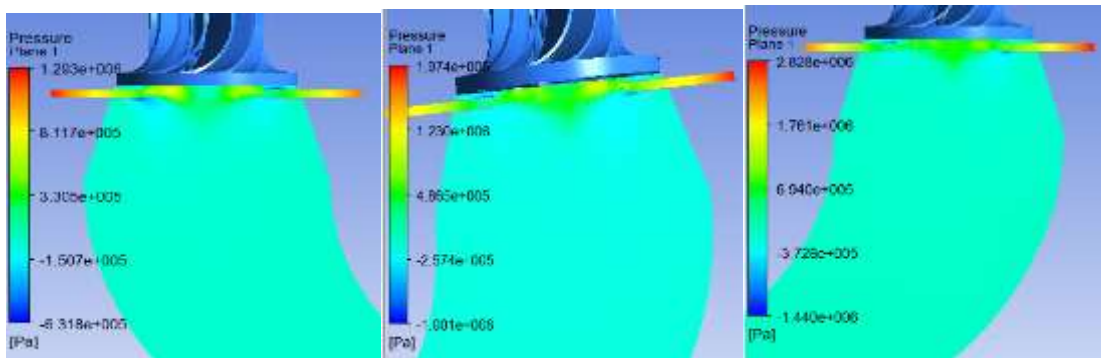
Pressure distribution along the draft tube mid-plane is shown in Fig. 4.5. The low pressure region generated at the draft tube center originates from the swirling flow leaving the runner. The vortex rope in the draft tube is generally wrapped around this low pressure region. Moreover, pressure gradient from center of the draft tube to the wall is large and it changes constantly with the runner angular movement. Low pressure zone at 50% Q_{BEP} the center of the runner outlet can be seen that correspond to the vortex core in figure below. The pressure contour plots show that the center vortex at lowest pressure contours in mid plane taps at the vertical outside of the turbine at figure (b).



(a) Q_{BEP}

(b) 50% Q_{BEP}

Without air admission (a) Q_{BEP} (b) 50% Q_{BEP}



0.3 Q_w

0.4 Q_w

0.6 Q_w

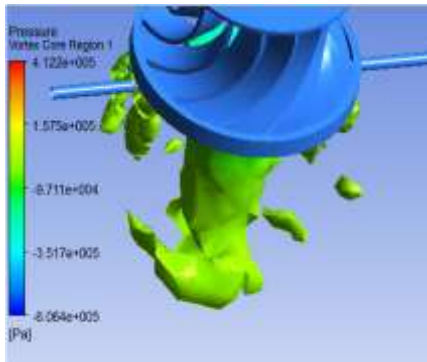
With air admission 50% Q_{BEP}

Fig. 4.5 Average pressure variation in the draft tube at cone operating condition; the pressure contours correspond to an instantaneous runner position at the end of unsteady simulation

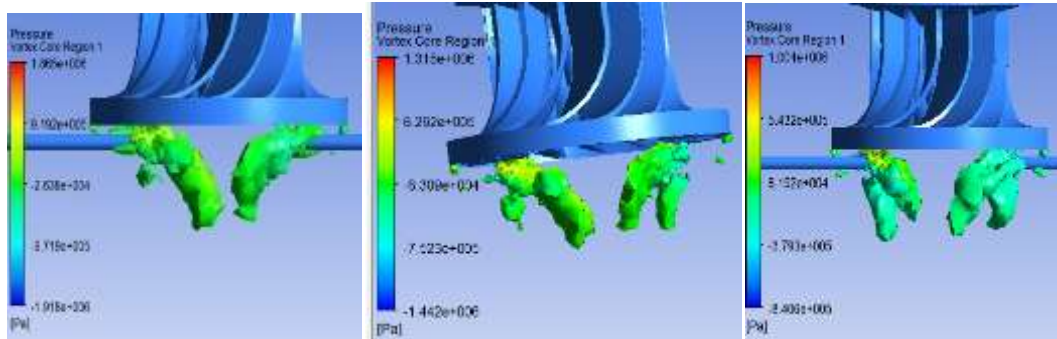
4.6.3 Vortex Rope with the Q-Criterion

Based on these results, the LES turbulence model is chosen for further unsteady simulations. Figure 4.6 compares the vortex rope resulting from these simulations with turbulent structures shown with the Q-criterion visualizations for 50% BEP. The vortex rope developed in 50% BEP is considerably larger both in diameter and length. As seen in this figure 4.6 It should be noted that simulation was performed for different cases (with and without air). However, regardless of the air admission.

Vortex rope in fig. 4.6 it can be seen, that for the locations of the the vortex rope for condition is almost in the center of the draft tube cone. The vortex has been found by applying the an iso surface with constant value for the Q-criterion on the simulation results. The Q-criterion is defined as positive second invariant for ∇u . It represents the local balance between shear strain rate and vorticity magnitude. Vortices are areas where the vorticity magnitude is greater than the magnitude of rate-of-strain.



(a) Vortex rope at 50% Q_{BEP}



(b)

(c)

(d)

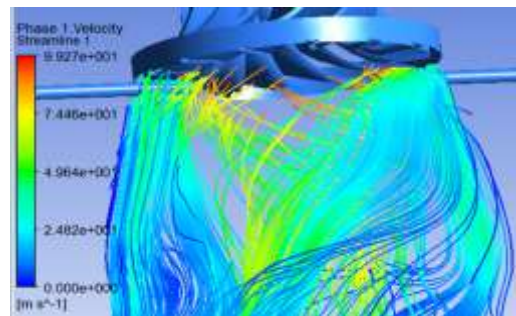
With air admission (b) $0.3Q_w$, (c), $0.4Q_w$ and (d) $0.6Q_w$

Fig. 4.6 Vortex rope with the Q-criterion

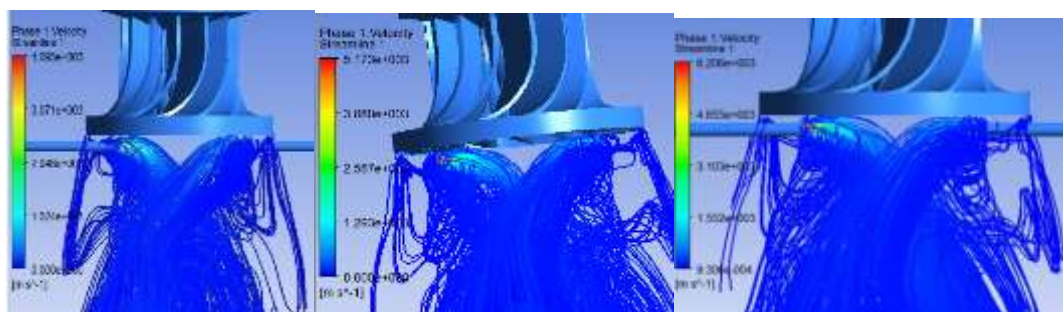
4.6.4 Velocity Streamlines Plane with Air Injection System 180°

A Streamline is the path that a particle of zero mass would take as it travels through the draft tube domain. The calculation of large numbers of streamlines in a large domain may take a long period of time. Therefore, it is advisable to start by plotting a small number of streamlines, and then increasing the number of streamlines until the best ratio of generation time vs. detail is found.

Figure 4.7 shows velocity streamlines through the draft tube cone starting at the runner outlet. The view is close to the runner and draft tube cone, to emphasize the flow difference at the runner outlet between the operating points. The figure clearly shows the difference in flow rotation at the runner outlet. The velocity streamlined across the cross-section of the draft tube is shown in Fig. 4.7 the shape of the streamlines indicates the rotating vortex rope inside the draft tube. At the inlet of the draft tube, the flow entered with high velocity, decreasing continuously towards the outlet of the draft tube.



Stream 50% Q_{BEP}



(b)

(c)

(d)

With air admission (b) $0.3Q_w$, (c) $0.4Q_w$ and (d) $0.6Q_w$

Figure 4.7: Velocity streamlines leaving the runner and across the cross section of the draft tube.

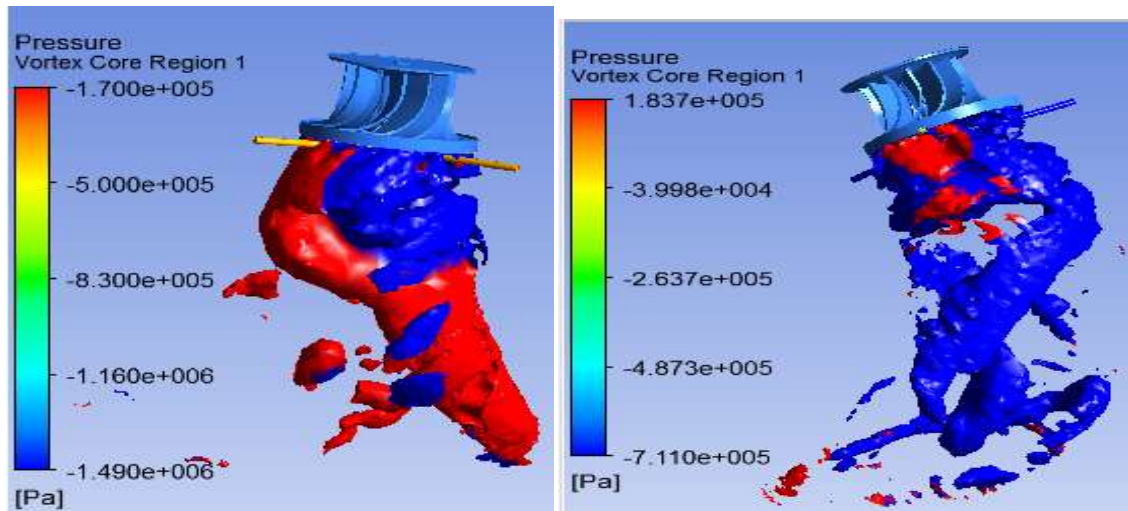
4.7 Air Injection System 120°

4.7.1 Vortex Rope with the Q-Criterion

As seen in this figure 4.8 (a) is the vortex rope is identified by Q criteria at $0.50 Q_{BEP}$ the resulting vortex rope has the shape of a rotating cork-screw. It should be noted that simulation was performed for different air pressures. However, regardless of the air admission pressure the vortex rope can be formed. From 1.10235 bar at figure (b) the vortex rope has the new shape of a rotation.

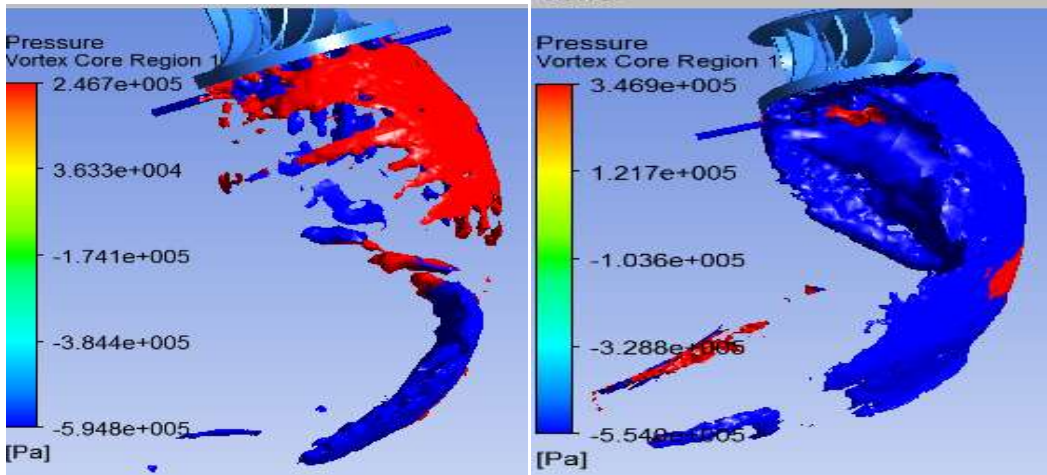
Figure (c) at 3 bar the vortex rope has reduced and water flow has the shape of draft tube

The physics behind the formation of a vortex rope is analyzed in this study is confirmed in the present simulations that the development of the vortex rope is associated with formation of a stagnant region at the center of the draft tube. This is mainly due to the wake behind the crown cone as well as the swirl, which tends to decrease flow momentum near the centerline. Comparison of the vortex rope shape observed at the different pressures.



(a) $0.50 Q_{BEP}$

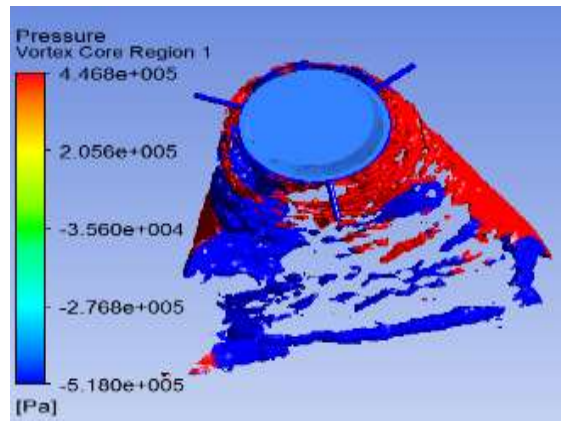
(b) 1.10235 bar



(c) 2 bar

(d) 3 bar

Fig. 4.8 Vortex rope with the Q-criterion (a), (b), (c) and (d)

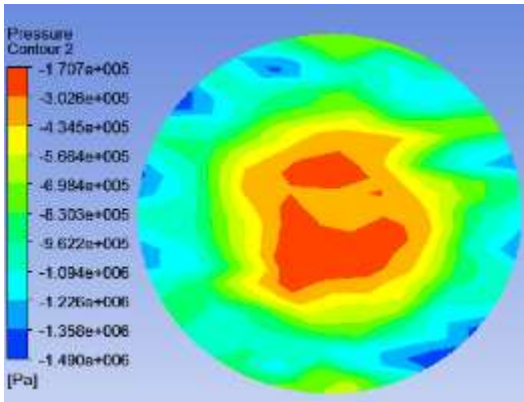


(e) 4 bar

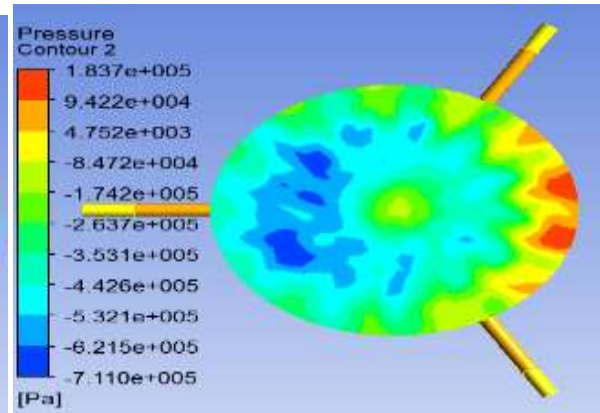
Fig. 4.8 Vortex rope with the Q-criterion(e)

4.7.2 Pressure Distribution at Draft Tube Inlet Horizontal Section

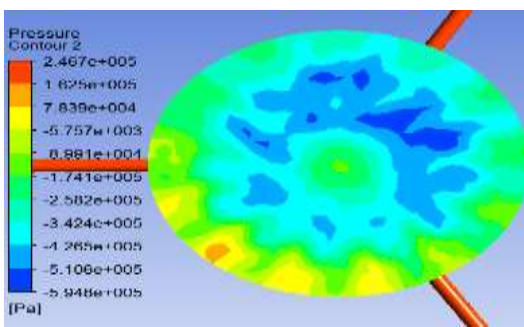
It can be found that under air supply condition 1.10235 bar at figure (b) denoting that air admission under this condition doesn't have any effect in pressure distribution but after injected 3 bar the contour pressure pulsations changed.



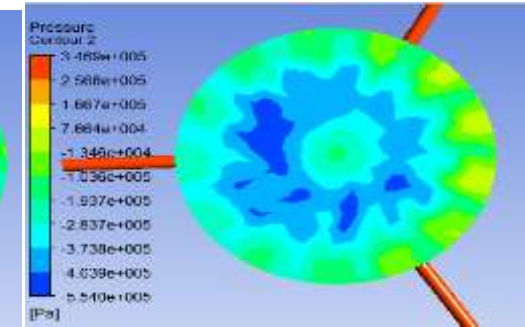
(a) 0.5QBEP



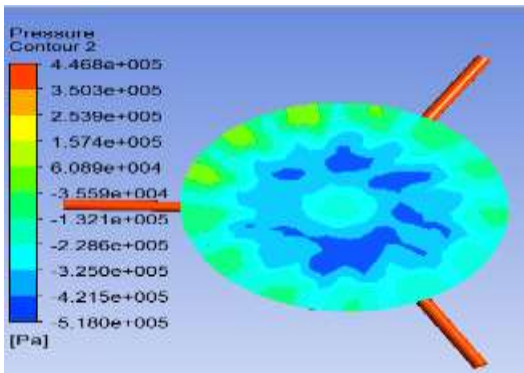
(b) 1.10235 bar



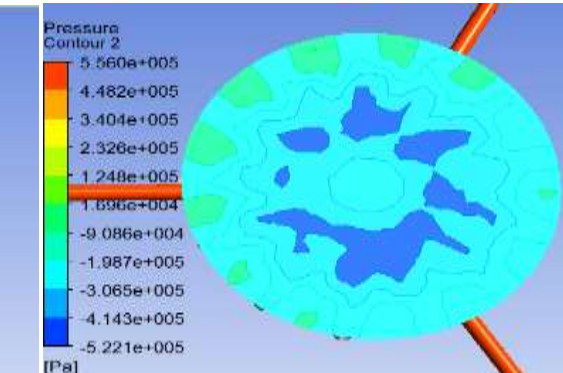
(c) 2 bar



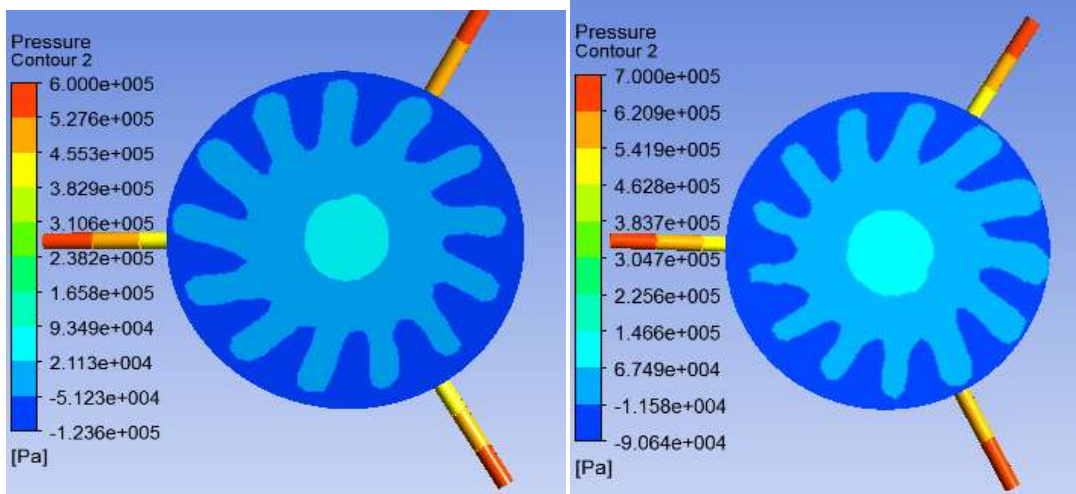
(d) 3 bar



(e) 4 bar

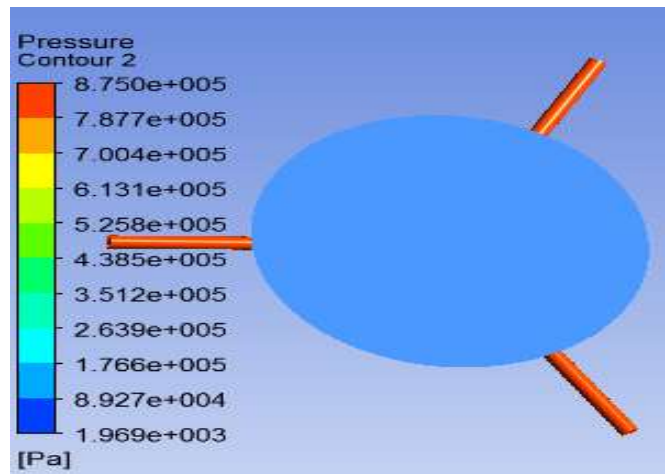


(f) 5 bar



(g) 6 bar

(h) 7 bar

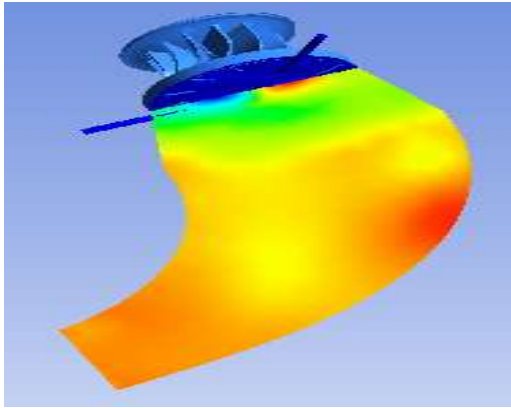


(i) 8 bar

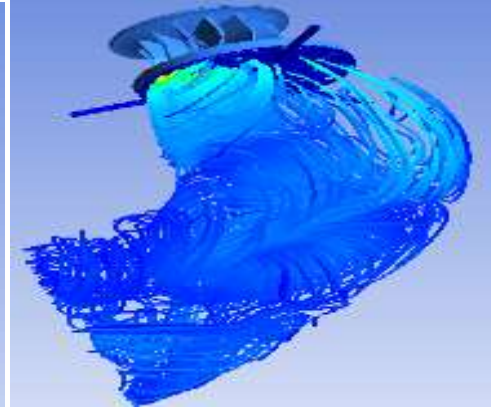
Fig. 4.9 pressure pulsations horizontal section

4.7.3 Draft Tube Vertical Section with Air Injection System 120°

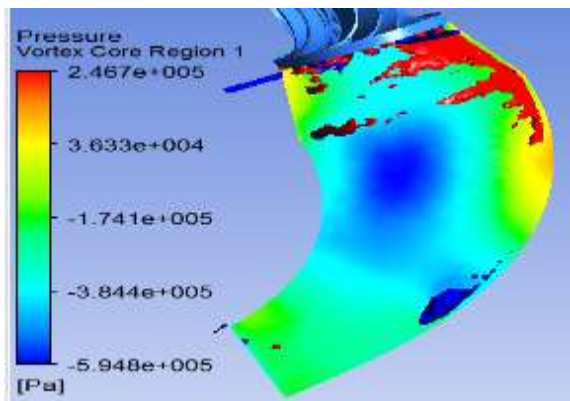
Fig. 4.10 depicts the relative pressure contours and Streamlines for different amounts of air Injection to the draft tube cone. It can be seen that, the shape of the low pressure zone below the runner cone varies with the amount of air injection.



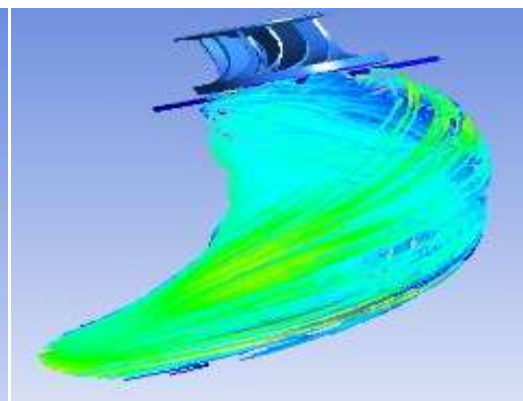
(a)



(b)

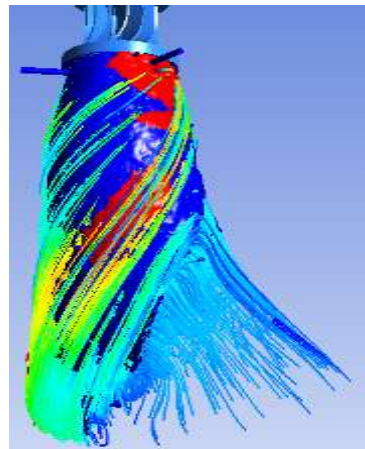


(c)



(d)

Fig. 4.10 draft tube vertical section with stream lines (a), (b), (c) and (d)



(e)

Fig. 4.10 draft tube vertical section with stream lines

4.8 Discussion of Amplitude (ΔH) and Pressure Pulsations ($\Delta H/H\%$)

4.8.1 Air Injection System 180°

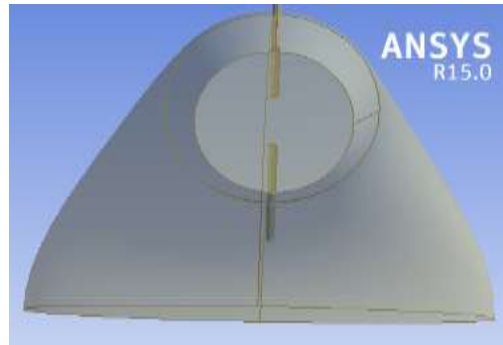


Table (4.5) Amplitude (ΔH) and pressure pulsations ($\Delta H/H\%$) At $0.5Q_{BEp}$ partial load with air admission System 180°

Ga. (deg)	Q(m ³ /s)	Air	ΔH		$\Delta H/H\%$	
			Without air	With air	Without air	With air
18.3	127.2	$0.3Q_w$	4.25	1.09	12.9%	3.3
18.3	127.2	$0.5Q_w$	4.25	0.846	12.9%	2.4
18.3	127.2	$0.6Q_w$	4.25	0.247	12.9%	0.7

4.8.2 Air Injection System 120°

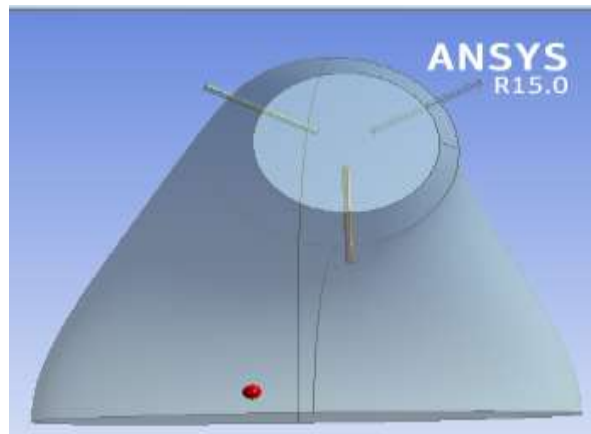


Table (4.6) Amplitude (ΔH) and pressure pulsations ($\Delta H/H\%$) At 0.5QBEP partial load with air admission System 120°

Ga. (deg)	Q(m ³ /s)	Pair (bar)	ΔH (m)		$\Delta H/H\%$	
			Without air	With air	Without air	With air
18.3	127.2	1.10235	4.077	2.77	12.36%	8.38%
18.3	127.2	2	4.077	2.09	12.36%	6.33%
18.3	127.2	3	4.077	1.95	12.36%	5.9%
18.3	127.2	4	4.077	1.79	12.36%	5.4%
18.3	127.2	5	4.077	1.00	12.36%	3.03%
18.3	127.2	6	4.077	0.09	12.36%	0.28%
18.3	127.2	7	4.077	0.7	12.36%	2.22%
18.3	127.2	8	4.077	0.27	12.36%	0.836%

4.8.3 Hill chart modification

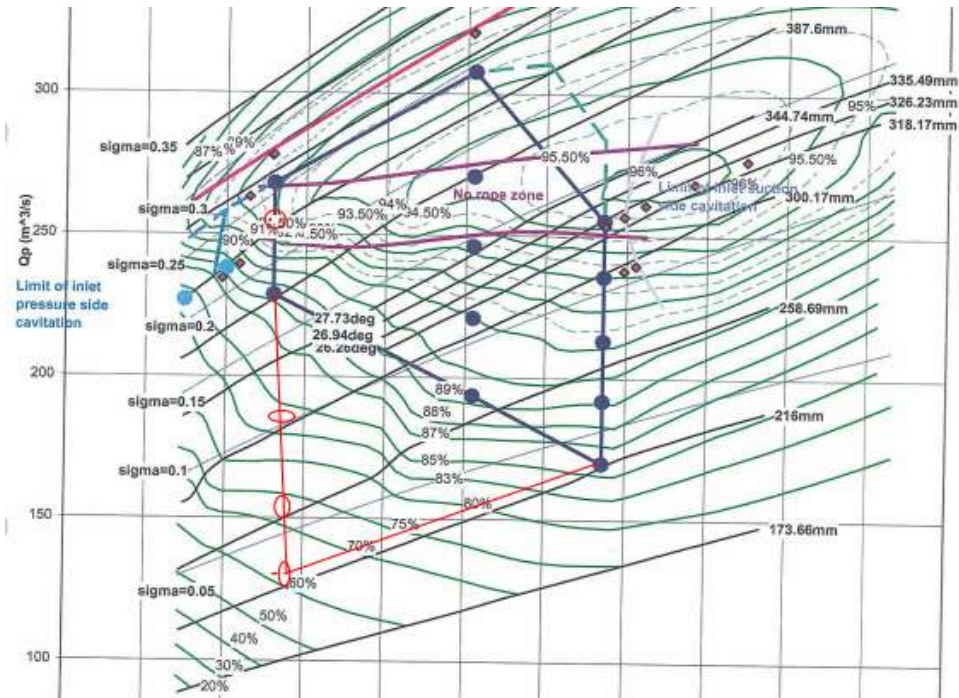
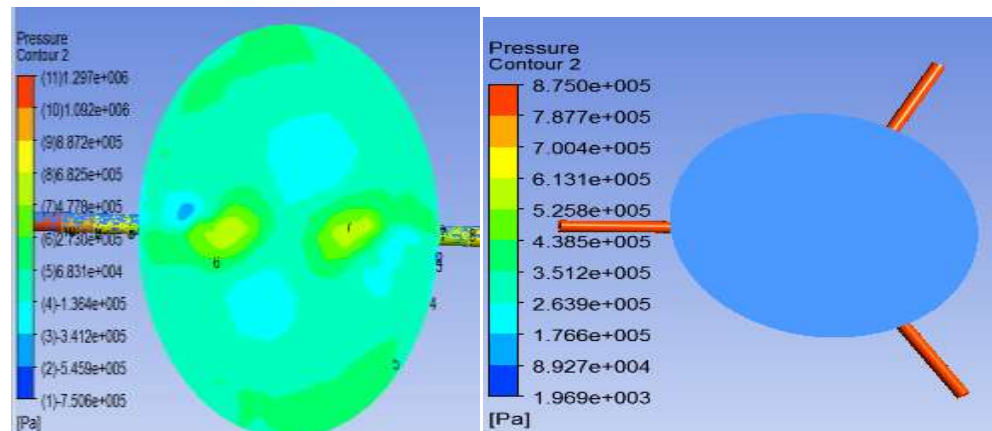


Figure 11. additional area on hill chart

4.9 Comparison Between Two Systems

High air pressure to eliminate lower pressure area cause efficiency losses and require a large power expenditure for the compressor when use System 180°



System 180°

System 120°

4.10 Summary

One of the main conclusions of this chapter is that the LES simulations can correctly predict the flow in the draft tube when the turbine is operating under partial load and the vortex rope forms inside the draft tube.

The prediction of pressure pulsations and vortex structures ejected by the runner in the draft tube inlet plane and mitigate by air admission through the cone wall using LES.

Chapter V
Conclusions and Recommendations

Chapter V

Conclusions and Recommendations

5.1 Highlights

The work presented in this partial PhD degree thesis aimed to investigate pressure pulsations and vortex cause of the Partial discharge during the commissioning of a Francis turbine runner at M.D. power plant. 3D models of the draft tube and runner geometry are created in Solid work and ANSYS CFD used structured mesh is created for the system simulation. Along the path of this extensive investigation, numerous findings and conclusions were drawn regarding certain physical and methodological aspects. The next few paragraphs aim to summarize briefly the principal conclusions of interest. Finally, have recommendations for farther research efforts in the field are also listed.

5.2 Conclusion

The main findings of this work can be subdivided based on the three principal objectives summarized in the Introduction and listed here again for reminder

In order to investigate the effect of air admissions to pressure pulsations simulated the three-dimensional unsteady flow in the Francis turbine draft tube at a part load operation condition. two monitoring sections in the draft tube are set horizontal section near the inlet of the draft tube is chosen and another is vertical section.

In order to alleviate the pressure pulsations induced and the vortex rope, air Injection to the draft tube cone wall is applied, and the water-air two phase flow in the entire flow passage of a model draft tube is simulated based on a homogeneous flow assumption and Large Eddy Simulation (LES) turbulence model.

1. Identify the physical mechanisms responsible of mixture (water and air) during the part load operation from 70% to 50% of the BEP flow rate and the physics behind it is understood. High fidelity numerical simulations are carried out using a turbulence models in the framework of LES modeling. The pressure pulsations in a draft tube operated at a part load condition are well predicted by the present numerical method.

2. When air pressure increase from 1.10235 bar to 4 bar, the pressure pulsations decreases a little, at 5 bar is suitable for operation during guaranteed, 8 bar the pressure pulsations will be alleviated.

3. The shape of vortex rope was changed with increase of air pressure, when the supplied air pressure is large the eccentric distance of vortex rope obviously at 4 bar fully distributed.

4. Admitting air to the draft tube cone through the wall is shown to be an effective method in mitigating the vortex rope formation, the shape of the runner and the draft tube and cannot be changed by air admission. With air admission, the pressure difference in the section of draft tube decreases, while the amplitude of pressure pulsation decreases at 1.10235 bar. Basically, the pressure pulsations change by air admission through cone wall.

5. The simulation results are compared with the ALSTOM guaranteed value data. Even though the simulations are performed with a phase flow, the cork screw shaped draft tube vortex appears at part load.

6. All these results make good expectations about the use of air injection for mitigation of the pressure pulsations and breakdown vortex at part load to improve operation area with different air flow injected and the same dimension of the hole of the injector.

5.3 Recommendations for Future Studies

This thesis is focalized on a way to use air injection method in a draft tube of a Francis turbine to mitigation of the pressure pulsations and breakdown vortex at part load to improve operation area with different air flow injected and the same dimension of the hole of the injector.

- To continue this work, multiphase simulations incorporating the effects of cavitations should be considered with mixture.
- The characteristics that the air bubbles must have to ensure a reduction of skin friction between a moving liquid and the wall where the liquid flows.
- Another aspect that could be study more, is the possibility to improve the dissolved oxygen in the water.
- Investigate the effect of air in turbine blades trail edge and effects of back-pressure.

- □ Re-optimize slit width and location of air injector with respect to different turbine blade operation and designs.
- An active air injection system and flow control method which injects air into the draft tube.

References

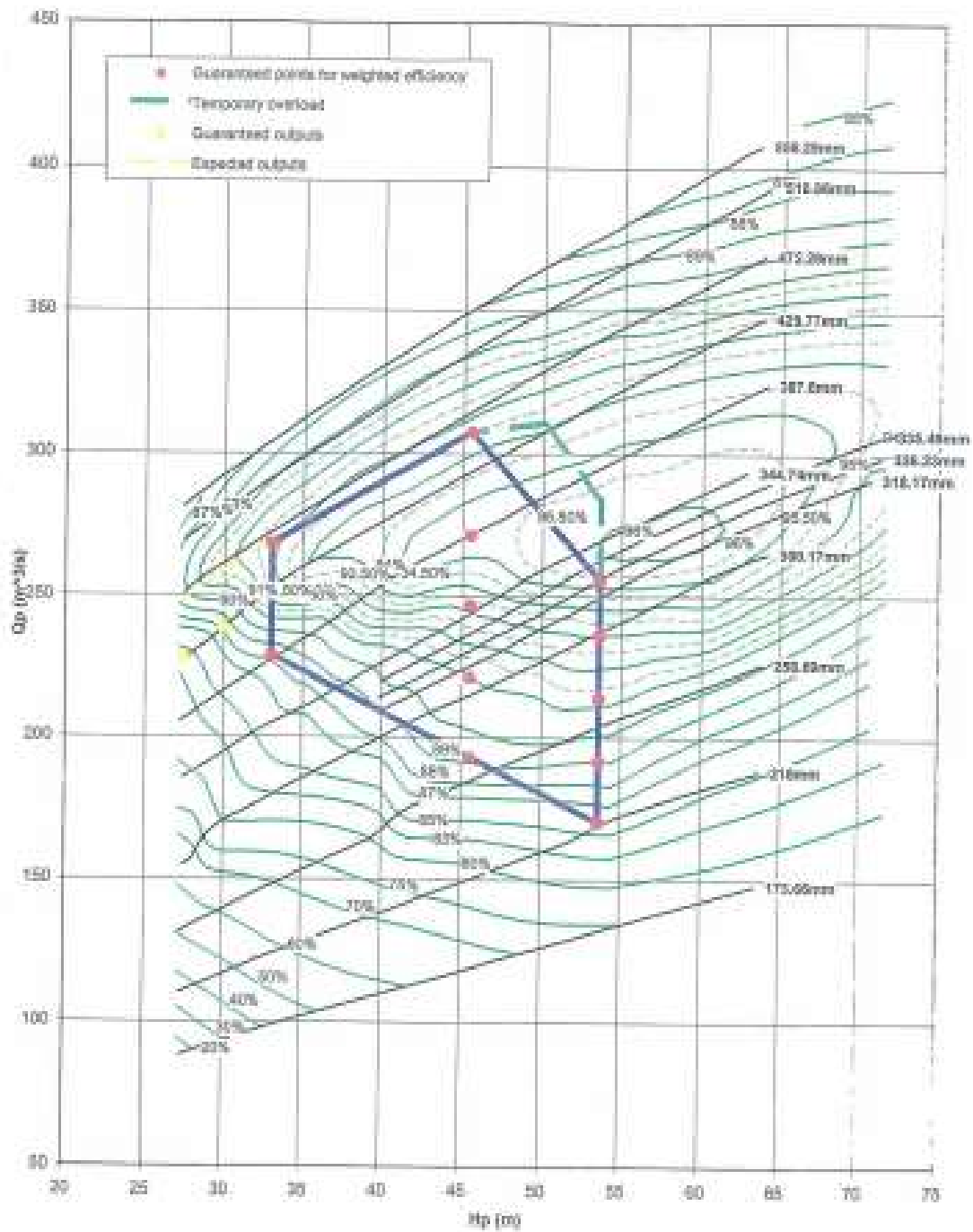
- A YU¹, X. W. L.,² AND B J³ 2015. Numerical simulation and analysis of the internal flow in a Francis turbine with air admission. *Materials Science and Engineering*.
- ADOLFSSON, S. 2014. Expanding operation ranges using active flow control in Francis turbines. *15HE credits*.
- AL, Y. T. E. 2014. Experimental and numerical investigation of unsteady behavior of cavitating vortices in draft tube of low specific speed Francis turbine. *27th IAHR Symposium on Hydraulic Machinery and Systems (IAHR 2014)*.
- ALIN I. BOSIOC¹, C. T., SEBASTIAN MUNTEAN², ROMEO F. SUSAN-RESIGA³ Number 3/2010,. PRESSURE RECOVERY IMPROVEMENT IN A CONICAL DIFFUSER WITH SWIRLING FLOW USING WATER JET INJECTION. *THE PUBLISHING HOUSE OF THE ROMANIAN ACADEMY*.
- ALLIGNÉ, S. 2011. Forced and Self Oscillations of Hydraulic Systems Induced by Cavitation Vortex Rope of Francis Turbines.
- ARTHUR FAVREL, J. G. P. J., CHRISTIAN LANDRY, ANDRES MÜLLER, CHRISTOPHE NICOLET & FRANÇOIS AVELLAN 2017. New insight in Francis turbine cavitation vortex rope: role of the runner outlet flow swirl number. *Journal of Hydraulic Research*, .
- BREIVIK, S. R. Juni 2011. CFD analysis of a runner and draft tube *Ole Gunnar Dahlhaug, EPT*.
- BRUNES, B. T. December 2009. Increasing power output from Francis turbines. *Norwegian University of Science and Technology*.
- C TANASA¹, S. M., T CIOCAN² AND R F SUSAN-RESIGA³ 2016. 3D Numerical Simulation versus Experimental Assessment of Pressure Pulsations Using a Passive Method for Swirling Flow Control in Conical Diffusers of Hydraulic Turbines. *Earth and Environmental Science 49 (2016)*.
- CIOCAN, G. D. 2007. Experimental Study and Numerical Simulation of the FLINDT Draft Tube Rotating Vortex. *Transactions of the ASME*.
- CONSTANTIN TĂNASĂ*, A. I. B., SEBASTIAN MUNTEAN**, ROMEO F. SUSAN-RESIGA* Number 2/2011. FLOW-FEEDBACK CONTROL TECHNIQUE FOR VORTEX ROPE MITIGATION FROM CONICAL DIFFUSER OF HYDRAULIC TURBINES DRAFT TUBE. *PROCEEDINGS OF THE ROMANIAN ACADEMY, Series A*,.
- DAQING 2016. Experimental study of the influence of Thoma number and model testing head on pressure fluctuation in draft tube of a Francis turbine. *28th IAHR symposium on Hydraulic Machinery and Systems (IAHR2016)*.
- DECAIX*, J. 2015. RANS COMPUTATIONS OF A CAVITATING VORTEX ROPE AT FULL LOAD. *6th IAHR International Meeting of the Workgroup on Cavitation and Dynamic Problems in Hydraulic*.
- DOERFLER, P. K. 02 June 2016. Observation of pressure pulsations at high partial load on a Francis model turbine with high specific speed>. *Conference Paper* .
- FANELLI, M. 19 Jan 2010. The vortex rope in the draft tube of Francis turbines operating at partial load: a proposal for a mathematical model. *Journal of Hydraulic Research*.


- FAY1, A. A. 2010. Analysis of low-frequency pulsations in Francis turbines. *Earth and Environmental Science* 12 (2010).
- FOROUTAN, H. 2015. SIMULATION, ANALYSIS, AND MITIGATION OF VORTEX ROPE FORMATION IN THE DRAFT TUBE OF HYDRAULIC TURBINES.
- GAVRILOV, A. A. June 28, 2016. Vortical structures and pressure pulsations in draft tube of a Francis-99 turbine at part load: RANS and hybrid RANS/LES analysis. *International Journal of Heat and Fluid Flow*.
- GOMES, J. 2017. Transposition of Francis turbine cavitation compliance at partial load to different operating conditions. *Journal of Physics: Conf. Series* 813 (2017) 012030.
- GUIDE, A. C.-S. T. December 2006. ANSYS CFX-Solver Theory Guide.
- GUIDE, A. C.-S. T. November 2013a. ANSYS CFX-Solver Theory Guide.
- GUIDE, A. F. T. November 2013b. ANSYS Fluent Tutorial Guide.
- HARRIS, M. J. April 2013. Flow Feature Aligned Mesh Generation and Adaptation. *University of Sheffield*.
- HELMRICH2, A. R. T. 2015. Simulation of pressure surge in a hydro power plant caused by an elbow draft tube. *IAHRSymposium Charlotte*.
- HUANG, R. August 3-7, 2014. NUMERICAL SIMULATION OF PRESSURE VIBRATIONS IN A FRANCIS TURBINEDRAFT TUBE WITH AIR ADMISSION. *Chicago, Illinois, USA*.
- ILIESCU, M. S. FEBRUARY 2008,. Analysis of the Cavitating Draft Tube Vortex in a Francis Turbine Using Particle Image Velocimetry Measurements in Two-Phase Flow. *Journal of Fluids Engineering*.
- J.PLADE, U. July 1972. Influence of draft tube shape on surging characteristics of reaction turbine.
- JEON, Y. .2014. Effect of Air Admission on Pressure Pulsation in a Francis Turbine. *New & Renewable Energy*.
- KAMKAR, S. J. February 2011. MESH ADAPTION STRATEGIES FOR VORTEX-DOMINATED FLOWS. *Re-distributed by Stanford University*.
- KAPOOR, H. 2014. Open Source Mesh Generation and CFD Simulations for Francis Turbine. *Chalmers University of Technology*.
- KIRSCHNER, O. October 24 - 26, 2007. VORTEX ROPE MEASUREMENT IN A SIMPLIFIED DRAFT TUBE. *IAHR International Meeting of the Workgroup on Cavitation and Dynamic Problems in Hydraulic Machinery and Systems*.
- KRANE, E. 2015. Simulations of the flow-driven rotation of the Francis-99 turbine runner. *CHALMERS UNIVERSITY OF TECHNOLOGY*
- KUIBIN, P. A. 2010. Validation of mathematical models for predicting the swirling flow and the vortex rope in a Francis turbine operated at partial discharge. *Earth and Environmental Science*.
- LIPEJ, A. September 9-11, 2015. Cavitation and dynamic problems. *Ljubljana, Slovenia*.
- M MELOT, B. N. A. N. D. 2014. Draft tube pressure pulsation predictions in Francis turbines with transient Computational Fluid Dynamics methodology. *Earth and Environmental Science* 22 (2014).

- MÜLLER, A. F. A. 2015. Study of the vortex-induced pressure excitation source in a Francis turbine draft tube by particle image velocimetry. *RESEARCH ARTICLE*.
- NICOLETI, J. A. C. 2009. Experimental Evidence of Hydroacoustic Pressure Waves in a Francis Turbine Elbow Draft Tube for Low Discharge Conditions. *Journal of Fluids Engineering*.
- NICOLET, C. July 2, 2004 Identification and modeling of pressure fluctuations of a Francis turbine scale model at part load operation. *Symposium on Hydraulic Machinery and Systems Stockholm – Sweden*.
- NISHI, M. 12 August 2015. Study on Swirl Flow and Surge in an Elbow Type Draft Tube. *Conference Paper*.
- O KIRSCHNER, A. R., E GÖDE AND S RIEDELBAUCH 2012. Experimental investigation of pressure fluctuations caused by a vortex rope in a draft tube. *Earth and Environmental Science*.
- PAVEL RUDOLF, P. D. 2010. A CONTRIBUTION TO STUDY OF THE SWIRLING FLOW.
- PAVEL RUDOLF, P. D. June 2006. MODEL OF PRESSURE PULSATIONS IN HYDRAULIC TURBINE DRAFT TUBE BASED ON LINEARIZED. *Meeting of WG on Cavitation and Dynamic Problems in Hydraulic Machinery and Systems*.
- RESIGA, R. 22 April 2017. Analysis and Prevention of Vortex Breakdown in the Simplified Discharge Cone of a Francis Turbine. *Journal of Fluids Engineering*.
- RUCHONNET, P. K. D. A. N. 2012. A statistical method for draft tube pressure pulsation analysis. *Earth and Environmental Science 15 (2012)*.
- S. G. SKRIPKINA, B., P. A. KUIBINA, B, AND S. I. SHTORKA, B October 17, 2014. The Effect of Air Injection on the Parameters of Swirling Flow in a Turbine Draft Tube Model. *Technical Physics Letters, 2015, Vol. 41, No. 7, pp. 638–640. © Pleiades Publishing, Ltd., 2015*.
- SCHILLING, M. V. M. A. R. 2012. Numerical simulation of pressure pulsations in Francis turbines. *Earth and Environmental Science 15 (2012)*.
- STOPPATO, A. 2014-15. AIR INJECTION IN THE DRAFT TUBE OF A FRANCIS TURBINE TO IMPROVE THE EFFICIENCY.
- SUSAN-RESIGA, R. JANUARY 2006. Analysis of the Swirling Flow Downstream a Francis Turbine Runner. *Journal of Fluids Engineering*.
- SUSAN-RESIGA, R. F., MUNTEAN, S., AVELLAN, F. & ANTON, I. 2011. Mathematical modelling of swirling flow in hydraulic turbines for the full operating range. *Applied Mathematical Modelling, 35, 4759-4773*.
- TØRKLEP, A. M. June 2012. Pressure oscillations during start and stop of a high head Francis turbine. *Norwegian University of Science and Technology Department of Energy and Process Engineering*.
- TRIDON, S. 2010. Experimental analysis of the swirling flow in a Francis turbine draft tube: Focus on radial velocity component determination. *elsevier*.
- VELI 2013. The vortex effect of Francis turbine in electric power generation. *Turkish Journal of Electrical Engineering & Computer Sciences*.
- VIKTOR ILIEV, P. P., ZORAN MARKOV December 2012. Transient Phenomena Analysis in Hydroelectric Power Plants at Off-Design Operating Conditions. *International Journal of Engineering Research*.
- W F LI, J. J. F. July-September 2015. Numerical Investigation of Pressure Fluctuation Reducing in

- Draft Tube of Francis Turbines. *International Journal of Fluid Machinery and Systems*, Vol. 8, No. 3,.
- WANG 2012. Numerical Simulation of Pressure Fluctuations in a Large Francis Turbine Runner. *CHINESE JOURNAL OF MECHANICAL ENGINEERING*.
- WANG, H. 2015. Analysis and control of the part load vortex rope in the draft tube of a pumpturbine. *Cavitation and Dynamic Problems in Hydraulic Machinery and Systems*", Ljubljana, Slovenia, September 9-11, .
- WRAY, T. Winter 12-15-2016. Development of a One-Equation Eddy Viscosity Turbulence Model for Application to Complex Turbulent Flows. *Washington University in St. Louis*.
- XIANWU LUO¹, A., BIN JI², YULINWU¹ AND YOSHINOBU TSUJIMOTO³ 2017. Unsteady vortical flow simulation in a Francis turbine with special emphasis on vortex rope behavior and pressure fluctuation alleviation. journals.sagepub.com/home/pia.
- ZHONG-DONG, Q. May 21, 2007. NUMERICAL SIMULATION AND ANALYSIS OF PRESSURE PULSATION IN FRANCIS HYDRAULIC TURBINE WITH AIR ADMISSION. *Journal of Hydrodynamics*
- ZUO August 13, 2014. Numerical predictions and stability analysis of cavitating draft tube vortices at high head in a model Francis turbine. *Science China Press and Springer-Verlag Berlin Heidelberg 2014*.

Appendix A : Merowe Hill Chart Efficiency



	14,000 Minutes Prototype HILL CHART - H_{tp} - Q_p and guaranteed points	ALSTOM Power
		Visé par: R. CHIAPPA Diagram No: 4.3 Date: 26/08/2004

Appendix B : Merowe Hill Chart Rope Zone

